3-23-2018

A Method to Determine the Viability of Photovoltaic Systems in Various Climate Regions

Joseph A. Applebee

A METHOD TO DETERMINE THE VIABILITY OF PHOTOVOLTAIC SYSTEMS

IN VARIOUS CLIMATE REGIONS

THESIS

Joseph A. Applebee, Captain, USAF

AFIT-ENV-MS-18-M-174

DEPARTMENT OF THE AIR FORCE
AIR UNIVERSITY

AIR FORCE INSTITUTE OF TECHNOLOGY

Wright-Patterson Air Force Base, Ohio

DISTRIBUTION STATEMENT A:
APPROVED FOR PUBLIC RELEASE; DISTRIBUTION UNLIMITED

The views expressed in this thesis are those of the author and do not reflect the official policy or position of the United States Air Force, the Department of Defense, or the United States Government.

AFIT-ENV-MS-18-M-174

A METHOD TO DETERMINE THE VIABILITY OF PHOTOVOLTAIC SYSTEMS IN VARIOUS CLIMATE REGIONS

THESIS

Presented to the Faculty

Department of Systems and Engineering Management

Graduate School of Engineering and Management

Air Force Institute of Technology

Air University

Air Education and Training Command

in Partial Fulfillment of the Requirements for the

Degree of Master of Science in Engineering Management

Joseph A. Applebee, BS

Captain, USAF

March 2018

DISTRIBUTION STATEMENT A:
APPROVED FOR PUBLIC RELEASE; DISTRIBUTION UNLIMITED

AFIT-ENV-MS-18-M-174

A METHOD TO DETERMINE THE VIABILITY OF PHOTOVOLTAIC SYSTEMS IN VARIOUS CLIMATE REGIONS

Joseph A. Applebee, BS
Captain, USAF

Approved:

Diedrich Prigge, PhD (Chairman)	Date
Alfred E. Thal, Jr., PhD (Member)	Date
Torrey Wagner, PhD (Member)	Date

AFIT-ENV-MS-18-M-174

Abstract

The purpose of this study is to manufacture and disseminate photovoltaic test systems which will be located at various United States Air Force installations worldwide. The Air Force's goals in renewable energy are to determine the potential for systems to aid in promoting resiliency for an installation's energy demands.

The overall goal of the data collection is to determine the correlation between power output of photovoltaic panels and the associated geographic region climate classification. The region's climate identification are determined using the Köppen-Geiger climate classification model. The test systems consist of two photovoltaic panels, monocrystalline and polycrystalline, and a control unit. Data is gathered and consolidated on a monthly basis to include power output, humidity, and internal/external temperatures.

This study does not include a complete analysis of the data as a full year of data has not yet been recorded. A full year of data, including all four seasons, is required for a proper analysis to be completed. Instead, the study highlights the manufacturing process, shipment of the systems, and associated limitations realized throughout these processes. Also, a partial year of data will be analyzed for initial observations. Some of the limitations realized include hardware malfunctions, lack of installation cooperation, and data gaps.

The conclusion which can be drawn from this study is that the test systems performed as expected. Not including hardware malfunctions, the systems were able to measure all data as designed. Analysis was able to be completed on four months data which provided initial results and observations on the climate region's performance.

Table of Contents

Page

List of Figures

Figure Page

List of Tables

A METHOD TO DETERMINE THE VIABILITY OF PHOTOVOLTAIC SYSTEMS IN VARIOUS CLIMATE REGIONS

I. INTRODUCTION

1.1 Background

The Department of Defense (DoD) has a vested interest in the use of renewable energy sources on its installations; they strive to find a system or method which provides energy resiliency, as well as continuing the push towards renewable energy. These safeguards would not only be used in austere environments, but also would help provide for the energy demand of DoD installations stateside. This desire pushes research initiatives and United States Air Force policy towards renewable energy initiatives. Furthermore, these directives help provide clarification on where and how responsible investment should be made in this field.

The purpose of this thesis is to study and analyze photovoltaic cells, a form of renewable energy, which harness the power of the sun by using light energy, or photons. The process of silicon material capturing photons results in the release of electrons which are then captured by conductive material placed within the photovoltaic array [9]. The photovoltaic arrays directs the energy created to a battery bank or electrical infrastructure.

The amount of energy photovoltaic cells produce is subject to a number of climatic variables. The effects of these variables on energy production is an ongoing topic in research efforts [17, 26, 44]. Some of these variables include but are not limited to temperature, humidity, precipitation, and climate classification. For the purposes of this study, the Köppen-Geiger climate classification system are used to classify regions in which United States Air Force (USAF) installations are located [28].

These classifications are analyzed by gathering data from the selected installations which were grouped by a Pareto analysis [10]. Test systems designed to gather photovoltaic energy production data, and climatic variables, will be sent to these specified locations. The data will then be gathered and analyzed on these climate regions to generate a conclusion on where USAF renewable energy infrastructure investment should be used and can be developed.

Installing a photovoltaic cell array large enough to generate sufficient energy return requires significant investments of both capital and land allocation. The current inability to accurately estimate the payback period of photovoltaic cells causes the first issue of capital investment. Currently, general estimates are used to predict energy production, which are not based upon specific climate regions but upon climatic effects such as temperature and humidity [9, 39, 44]. The United States Air Force faces the question of land allocation, a problem preventing photovolatic cell array development. The majority of Air Force land ownership centers around the flightline area including runways, taxiways, and aprons. This land is not allowed to have structures built upon it due to the existing Federal Aviation Administration (FAA) and United States Air Force policies and regulations on clear zones for the surrounding areas [1]. This means that though the USAF may have vast amounts of empty land, much of that acreage is unsuitable for construction. Therefore, it is important to justify the specific amount of land needed for installations to produce the energy required.

Once a suitable amount of acreage is identified, installations will be able to make an informed decision on whether a photovoltaic array is viable.

1.2 Problem Statement

The United States Air Force's use of photovoltaic cells is not a new concept. One of the many current installations utilizing this technology is Nellis Air Force Base (AFB). After Nellis AFB granted a portion of its land to a private energy company for the construction of a large solar array, it now receives a discounted energy rate from Nevada Energy for a period of 20 years. The 14.2-megawatt solar array, with 70,000 panels, was the largest in the United States at the time of its unveiling [15]. This private business partnership is one of the few avenues the DoD currently uses to utilize energy from renewable sources. However, the large success realized from this project creates momentum toward new renewable energy projects for the DOD. Nellis AFB has recently constructed a second solar array with the capacity of 19 megawatts, that coupled with the first, will now be able to completely power Nellis AFB during daytime operations [33].

DoD installations face the problem of determining where and how to invest in renewable energy. These avenues not only have to be financially viable, but they also must be able to produce enough energy to meet the installation's energy requirements to achieve the main goal of resiliency. Therefore, being able to develop a model which predicts energy production accurately is necessary to determine lifetime costs, payback periods, and energy production potential [4, 14, 22, 27].

1.3 Research Objectives and Investigative Questions

The objectives of this research effort is to determine the viability of the Photovoltaic test systems described. This analysis examines the materials and construction methods used in the production of the systems. Also, the ability of the systems to gather data which is complete and usable on an ongoing basis is determined. This research highlights the abilities of the systems, as well as its limitations, for the use of future researchers. The following questions represent the goals of this research effort:

1. What level of data consistency will be gathered from the selected test sites?
2. What strategies need to be implemented to limit the effect of potential future hindrances on this study?
3. What analysis method should be used to find the viability of photovoltaic systems in various climate regions after a comprehensive data set is collected?

1.4 Methodology

The study is completed by gathering energy production data from 37 test sites around the globe [10]. The sites were chosen based on their varying climate regions defined through the Köppen-Geiger climate classification system [28, 43]. The classification system has a total of 30 distinct climate regions [28]. For the purposes of this study, the climate regions and associated number of test systems at those classifications can be seen in Table 1.1.

This study was a continuation of research completed by Nussbuam [10]. This previous effort accomplished system design and material procurement for the study. A Pareto analysis determined the test site locations by analyzing the location and climate regions

Köppen-Geiger Climate Classifications	Total Installation Count	Installation Pareto Analysis	Total Test Site Count	Test Site Pareto Analysis
Arid/Steppe/Cold Arid	613	34.77	6.00	16.67
Warm Temperate/Fully Humid/Hot Summer	340	19.29	4.00	11.11
Snow/Fully Humid/Warm Summer	307	17.41	4.00	11.11
Warm Temperate/Fully Humid/Warm Summer	97	5.50	2.00	5.56
Warm Temperate/Summer Dry/Warm Summer	82	4.65	3.00	8.33
Snow/Fully Humid/Hot Summer	55	3.12	3.00	8.33
Snow/Fully Humid/Cool Summer	54	3.06	2.00	5.56
Warm Temperate/Summer Dry/Hot Summer	49	2.78	2.00	5.56
Arid/Desert/Cold Arid	17	0.96	0.00	0.00
Arid/Steppe/Hot Arid	16	0.91	2.00	5.56
Polar//Polar Tundra	12	0.68	2.00	5.56
Arid/Desert/Hot Arid	11	0.62	2.00	5.56
Snow/Winter Dry/Hot Summer	11	0.62	2.00	5.56
/Fully Humid/	10	0.57	2.00	5.56
/Summer Dry/	10	0.57	0.00	0.00
Snow/Summer Dry/Warm Summer	7	0.40	0.00	0.00
/Monsoonal/	5	0.28	0.00	0.00
Snow/Summer Dry/Cool Summer	3	0.17	0.00	0.00
/Winter Dry/	3	0.17	0.00	0.00
Warm Temperate/Winter Dry/Hot Summer	2	0.11	0.00	0.00
Snow/Summer Dry/Hot Summer	1	0.06	0.00	0.00
Snow/Winter Dry/Warm Summer	1	0.06	0.00	0.00
Warm Temperate/Fully Humid/Cool Summer	1	0.06	1.00	2.78

Table 1.1: Test Site Climate Classifications [10]

of all USAF installations. Furthermore, the equipment had been selected and procured leaving only fabrication and testing to be completed. The test system programming had been written and tested using test models of the system housed at the Air Force Institute of Technology (AFIT)[10].

The data will be gathered monthly via email from the installation persons of contact (POC). The data contains measurements of voltage and amperage of both panels, taken at fifteen minute intervals. It also holds climatic data including temperature and humidity readings taken at the same interval.

A logistical analysis will be completed once data has been gathered from the test sites. The analysis compares the energy produced from each test site to its associated climate region. By comparing test site climate classifications, certain regions will be identified as most suitable and least suitable for energy production based upon the relationship strength between the climate classification and the energy production is what makes this distinction [9].

The equipment was sent to the 37 chosen sites in May 2017. The equipment being used is a combination of one 25 watt (mono-crystalline) and one 50 watt (poly-crystalline) photovoltaic cells. Each cell is connected to a control unit which houses the hardware to monitor and record the energy production of each cell. The cells will placed flat at all sites. This was done to ensure consistency of measurements during analysis. This software is powered by a Raspberry Pi ™, a small on-board computer processor. The Electrical Engineering Department at the Air Force Institute of Technology (AFIT) custom wrote/created the software for this analysis.

The contents of the control unit includes multiple probes, which monitor internal temperature, external temperature, and humidity level. This data, along with the respective cell's energy production, is recorded continuously at fifteen minute intervals continuously. A RockBlock™, a satellite controller, is also included in the control unit to give daily updates on the system's status.

1.5 Assumptions and Limitations

The installations were chosen based upon their differing climate regions. However, given the limitations of funding and available test sites, certain climate regions will not be studied. These areas are generally located in the polar and snow regions with no significant United States Air Force presence. Due to the geographic extent of this study, all of the test systems will be operated by volunteers located at the selected installations. Therefore, the high turnover rate of these United States Air Force personnel could lead to operation difficulty and potential loss of data.

II. LITERATURE REVIEW

2.1 General Issue

Photovoltaic technology has the opportunity to forever change the landscape of energy use within the United States Air Force. Therefore, it is becoming increasingly important to examine this renewable energy production method. This opportunity is specifically important because the United States Air Force accounts for approximately 48% of the energy used within the entire Department of Defense as can be seen in Figure 2.1[18]. This data combines total fuel use and electricity consumption into a single energy metric. Though the majority of this energy use is attributed to flight line operations, with the majority being fuel at approximately 81%, Air Force facility energy consumption can be calculated as 16% of the entire Department of Defense usage. This large energy consumption has prompted the Air Force to create a number of priorities to follow in the desire to reduce overall energy consumption [14]. These directives, stated in the United States Air Force Strategic Energy Plan, can be seen in Table 2.1.

The main goal of the United States Air Force in relation to renewable energy is the potential for increased resiliency. The USAF will continue to have a large energy demand due to the nature of its mission for years to come. The vast majority of USAF energy demand comes from petroleum. Therefore, the methods and practices which are required to produce and store this energy leave the USAF incredibly vulnerable. The supply chain network which is required to maintain the readiness posture of United States Air Force installations, faces the potential for attack on many levels. Because of this, the United

AIR FORCE ENERGY STRATEGIC PLAN		
PRIORITY	**INTENT**	**EXPECTED OUTCOME**
Improve Resiliency	↗ Identify vulnerabilities to energy and water supplies, such as physical and cyber attacks or natural disasters ↗ Mitigate impacts from disruptions in energy supplies to critical assets, installations, and priority missions	↗ Improved responsiveness to disruptions to energy and water supplies ↗ Increased ability to quickly resume normal operations and mitigate impact to the mission ↗ Prioritized response plans and solutions to mitigate risk from the tail (logistics supply chain) to the tooth (energy demand in operations)
Reduce Demand	↗ Increase energy efficiency and operational efficiency for Air Force systems and processes without losing mission capabilities	↗ Decreased amount of energy required by Air Force systems and operations ↗ Increased flexibility, range, and endurance in all operations
Assure Supply	↗ Integrate platform-compatible alternative sources of energy ↗ Diversify drop-in sources of energy ↗ Increase access to reliable and uninterrupted energy supplies	↗ Access to backup energy resources and supply chains based on asset and mission priorities ↗ Increased flexibility in all operations ↗ Increased ability to sustain mission
Foster an Energy Aware Culture	↗ Integrate communication efforts using training and education opportunities to increase awareness of energy impacts to mission ↗ Ensure the acquisition process reflects energy as a mission enabler	↗ Increased understanding and awareness of energy and its impacts to the mission ↗ Reduced energy demand through more efficient uses of energy resources ↗ Increased ability to integrate energy considerations in planning activities and other decisions

Table 2.1: Air Force Strategic Plan Energy Priorities [14]

States Air Force is actively looking at renewable energy sources to provide increased energy security and resiliency [14].

Furthermore, budgetary concerns are of growing interest to the USAF as well. As of 2011, the USAF allocated 11% of its total budget to energy as can be seen in Figure 2.1 [18]. The annual cost of energy and its continued rise have prompted the desire for change. The need for a stable and cost-effective alternative will help considerably in lowering the budget allocation and the annual costs [10]. For these reasons, the federal government

Figure 2.1: DoD/Air Force Energy Usage [18]

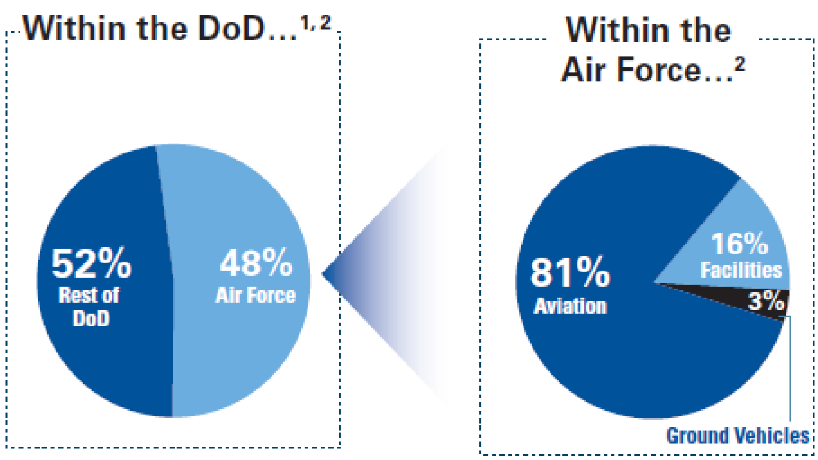

mandated that the DoD energy portfolio for facilities will be 25% renewable by the year 2025 [18, 46]. A plan created by the Air Force Civil Engineer Center (AFCEC) to attain the 25% goal can be seen in Figure 2.2.

Figure 2.2: Renewable Energy Goals [18]

Renewable Power Goal Under 10 U.S. Code 2911
Renewable Energy Electricity Requirements (MWh)

	FY13	FY14	FY15	FY16	FY17
RE goals	13%	14%	15%	16%	17%
RE electricity required (MWh)	1,179,155	1,257,161	1,333,488	1,408,164	1,481,212

Mechanisms to Reach RE Goals (MWh)

	FY13	FY14	FY15	FY16	FY17
On-base RE (carried fwd)	446,261	552,142	723,357	1,363,230	1,830,971
ECIP/SRM/ARRA (new on-base)	9,916	32,018	6,341	11,083	6,246
PPA RE (new on-base)	95,966	127,151	376,251	141,299	77,614
EUL RE (new on-base)	0	12,045	257,281	315,360	0
Commercial Bundled RE Purchase	54,899	54,899	54,899	169,899	169,899
Totals	607,041	778,256	1,418,129	2,000,870	2,084,730

EUL = Enhanced Use Lease, ECIP = Energy Conservation Investment Program, PPA = Power Purchase Agreement, SRM = Sustainment Restoration & Modernization

2.2 Current United States Air Force Utilization

The Department of Defense has been making strides in investment into solar capacity at many installations worldwide. As of 2013, there were more than 130 Megawatts of PV arrays located across all three services with 40 Megawatts belonging specifically to the USAF [46]. With the steadily decreasing price of PV systems, more than 40% since 2011, the DoD is finding itself with a large opportunity for smart investment. There are three ways which the military has used in the past to finance renewable energy projects. The first, a power purchase agreement, was previously referenced in terms of the two successful Nellis AFB projects which currently provide enough energy for all daytime operations [15, 33]. This agreement is a prearranged contract in which the private utility company agrees to sell energy at a fixed utility rate to the installation at no upfront cost to the government. For example, Nellis AFB allowed multiple solar arrays to be built upon their land in exchange for fixed utility rates for a period of 20 years [15, 33].

The second way in which the military has used private business to leverage their renewable energy production is through enhanced lease agreements. This method allows private business to lease government-owned land in exchange for rental payments. The benefit of this agreement for the government is that they receive income from the leased land as well as being able to use renewable energy, which has been fed back into the existing electrical grid [46].

The last way of investment is through energy savings contracts. These contracts allow the government to procure renewable energy projects at no upfront cost [46]. The private business, however, will receive payments based upon the estimated energy savings the installation will encounter.

2.3 PV Background

Solar cells, or photovoltaic (PV) cells, are a device which harnesses the power of sunlight to create electricity. This process can be completed using different materials, but the overall procedure remains the same. When light hits certain materials, free flowing electrons are released and captured by conductive conduits. These conduits are able to gather these electrons and ferry them to whichever energy system is being used. These can be anything from open circuits powering various systems to battery banks harnessing the energy for future use [34, 38].

Four major types of solar cells are poly-crystalline, mono-crystalline, amorphous, and organic cells [34]. For the purposes of this research, the two types which will be used are poly-crystalline and mono-crystalline. These two types of cells are the most widely used and available cells on the open market, approximately 90% of the available market share [45]. Poly-crystalline cells are made up of multiple silicone crystals. Raw silicone is melted into ingots which are then sliced to create the cells. Poly-crystalline cells are generally less efficient then mono-crystalline cells which are created by raw silicon being processed and then sliced to form cells [45].

Figure 2.3: Sample PV System [9]

The material used to create PV cells can be copper, cadmium sulphide, gallium arsenide, cadmium telluride, and silicon. Of all these materials, silicon presents the most benefit in energy production due to its price, availability, and energy production potential [34, 38]. PV cells can be arranged either as a single cell or in a series. Because a typical PV cell can only produce on average three Watts at 0.5 volts, a series system with multiple cells is generally used. The three types of silicon which are commonly used are amorphous, crystalline (Mono), and multi-crystalline (Poly). Amorphous (uncrystallized) silicon is the most popular thin-film technology with cell efficiencies of 5-7% and double- and triple-junction designs raising it to 8-10% [38]. Crystalline silicon offers an improved efficiency when compared to amorphous silicon while still using only a small amount of material. The commercially available poly-crystalline and mono-crystalline silicon solar cells have an efficiency around 15-20% and 24-28% respectively [19, 38, 51].

Increasing efficiency, reducing cost and minimizing pollution are benefits of photovoltaic systems that have led to the wide range of applications [38, 39]. These applications can range from large facility systems to home use systems, as well as more specific cases such as space applications. Building-integrated photovoltaic systems incorporate photovoltaic properties into building materials such as roofing, siding, and glass, thus offering advantages in cost and appearance as they are substituted for conventional materials [38, 40, 41].

These applications do not come without limitations. A few of the main issues affecting photovoltaic systems include storage and the varying energy production of the systems [21, 50]. In terms of storage, the ability to store energy in battery banks faces problems with efficiency and the large associated costs. This issue is especially important to the

United States Air Force given their main goal of resiliency. To maintain resiliency, some sort of storage system will need to be installed to ensure energy is available at any time. Currently, because of the problems associated with storage, many photovoltaic systems feed directly into the existing electrical grid, there by bypassing the storage option. This, of course, limits when a system may be utilized: only during daytime. Along those same lines, the effects of climatic conditions may negatively affect the ability to produce energy on a consistent basis. Large amounts of rain and cloud cover will limit the production and force the grid to rely on other energy sources [38].

2.4 Modeling Techniques

The ability to distinguish climate regions relies upon each regions unique climatic effects. These include variables such as temperature and humidity. Therefore, it is important to research the current literature on these individual characteristics and the effects they have on PV efficiency. Additionally, the current model's ability to accurately predict energy production will be needed to analyze similar techniques used in this study.

The desire to accurately predict how well a PV system will perform is not new. Numerous models have been created in which different variables have been used in varying ways to best predict efficiency. One of these studies, completed at Sandia National Laboratories by the Department of Energy (DoE), analyzed four radiation models, three module performance models, and an inverter model [25, 26, 29]. The study used three separate micro-grid PV systems to gather data on actual energy production. Once gathered, the weather data was entered into these different models to determine how closely the predicted energy data matched the real energy production. The DoE developed a new model for this comparison, PVWatts. PVWatts was found to be the most accurate model in predicting PV power production [32].

The DoE study found that the eight models that were analyzed did accurately predict energy production to a reasonable level as seen in Figure 2.4 and Figure 2.5. Though these results do prove existing models' ability to perform, doubts exist. Certain questions could be asked as to the worldwide application of this study. The study was completed in Albuquerque, NM, a climate which has low variability of climatic effects annually. Furthermore, all three micro-grid systems used, though in different configurations, were located in the same location with the same setup. The DoE references and acknowledges this lack of location and climate variability in their study as possible elements of concern and future research possibilities [12, 25, 26, 45].

A similar study was completed by the National Institute of Standards and Technology in 2009 which evaluated the previously stated Sandia Laboratories models with varying PV materials [9]. This included variations such as mono-crystalline, poly-crystalline, insulation, and glazing on PV systems. The results, shown in Figure 2.2, were similar to those of the DoE study in that the model predictions proved to be accurate to a reasonable level. Five of the six systems measured were consistently within 4% or better of the predicted models. However, a lack of location and climate variability was also present in this study since the testing systems were located in only one location in Maryland. This lack of variability in climate could hinder the ability to extrapolate the results to sites around the world [9].

Figure 2.4: PV Model Annual Performance - Actual vs Predicted [25]

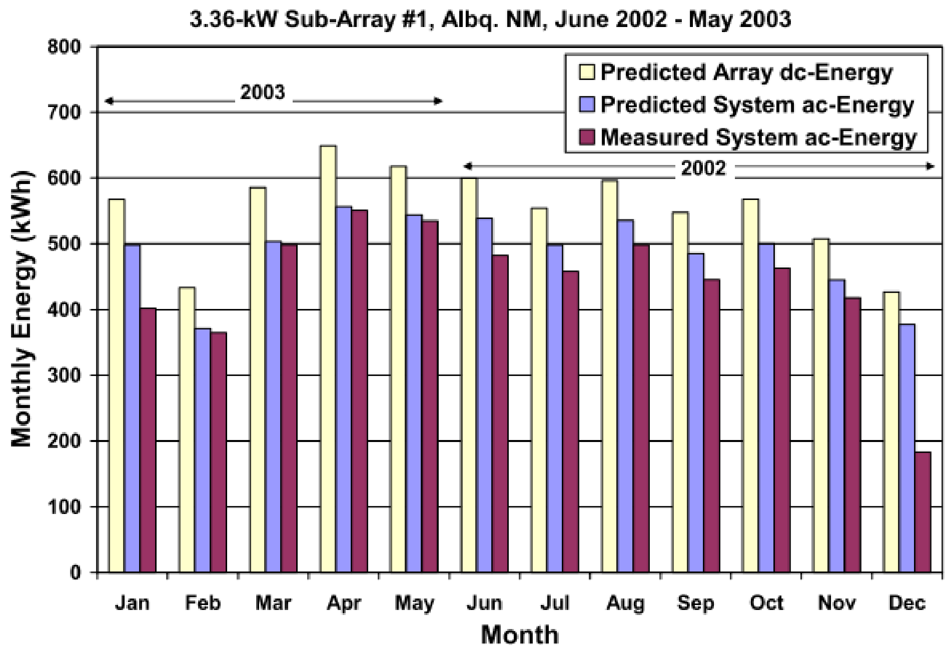

Figure 2.5: PV Model Efficiency Study - DOE [26]

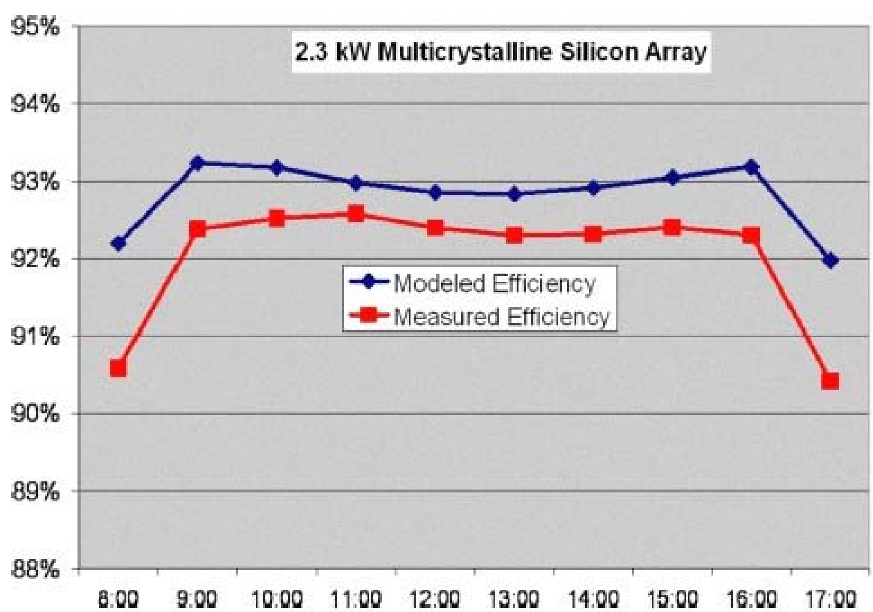

Module ID	A			B			C			D			E			F			G			H		
Cell type	Single crystalline			Polycrystalline			Polycrystalline			Polycrystalline			2-a-Si			2-a-Si			CIS			CIS		
Glazing	Glass			Glass			ETFE			PVDF			Glass			Glass			Glass			Glass		
Insulated	Yes			Yes			Yes			Yes			No			Yes			No			Yes		
Month	Meas. (kW h)	Pred. (kW h)	% diff.	Meas. (kW h)	Pred. (kW h)	% diff.	Meas. (kW h)	Pred. (kW h)	% diff.	Meas. (kW h)	Pred. (kW h)	% diff.	Meas. (kW h)	Pred. (kW h)	% diff.	Meas. (kW h)	Pred. (kW h)	% diff.	Meas. (kW h)	Pred. (kW h)	% diff.	Meas. (kW h)	Pred. (kW h)	% diff.
January	10.62	10.40	2.05	12.10	12.17	−0.54	13.06	12.88	1.42	13.18	13.02	1.27	6.27	7.83	−24.87	6.24	7.65	−22.72	13.77	12.87	6.59	13.18	12.37	6.15
February	11.10	10.77	2.99	12.61	12.47	1.07	13.57	13.21	2.68	13.71	13.32	2.87	6.52	7.88	−20.87	6.52	7.74	−18.68	14.22	13.22	7.01	13.62	12.78	6.20
March	9.80	9.33	4.83	10.85	10.40	4.12	11.77	11.19	4.92	11.77	11.26	4.34	5.55	6.44	−16.09	5.60	6.35	−13.39	12.09	11.29	6.58	11.77	11.04	6.17
April	9.69	9.12	5.87	10.65	10.00	6.09	11.58	10.88	6.04	11.56	10.96	5.19	5.55	6.11	−10.04	5.58	5.98	−7.21	11.86	11.21	5.51	11.47	10.91	4.93
May	7.36	7.05	4.09	7.93	7.46	5.93	8.67	8.27	4.70	8.60	8.37	2.63	4.05	4.50	−11.12	4.11	4.44	−7.96	8.79	8.64	1.70	8.54	8.47	0.81
June	7.03	6.82	3.06	7.55	7.04	6.69	8.28	7.94	4.15	8.16	8.07	1.15	4.00	4.35	−8.81	4.01	4.25	−5.77	8.41	8.46	−0.62	8.10	8.23	−1.60
July	7.36	7.24	1.60	7.97	7.58	4.96	8.74	8.49	2.86	8.64	8.62	0.26	4.30	4.71	−9.63	4.28	4.58	−6.90	8.97	9.08	−1.18	8.60	8.77	−2.01
August	7.91	7.83	0.96	8.72	8.46	2.89	9.52	9.32	2.05	9.46	9.43	0.30	4.77	5.26	−10.21	4.73	5.10	−7.64	9.85	9.86	−0.14	9.35	9.02	3.55
September	9.68	9.48	2.01	10.96	10.70	2.43	11.86	11.54	2.77	11.91	11.65	2.18	6.00	6.72	−12.02	5.94	6.47	−8.95	12.45	12.05	3.24	11.67	11.46	1.80
October	6.98	6.72	3.78	7.93	7.63	3.80	8.54	8.19	4.09	8.58	8.31	3.25	4.22	4.87	−15.45	4.22	4.72	−11.92	8.94	8.48	5.15	8.43	8.10	3.90
November	7.89	7.70	2.34	8.96	8.85	1.30	9.67	9.43	2.44	9.72	9.50	2.25	4.56	5.65	−23.94	4.59	5.52	−20.18	10.14	9.49	6.37	9.69	9.16	5.53
December	9.20	9.01	2.08	10.58	10.52	0.58	11.35	11.13	1.94	11.49	11.25	2.05	5.22	6.73	−28.93	5.27	6.63	−25.86	11.90	11.04	7.18	11.41	10.70	6.19
Total	104.62	101.49	3.00	116.81	113.28	3.02	126.62	122.46	3.28	126.79	123.75	2.39	61.00	71.05	−16.47	61.09	69.42	−13.63	131.39	125.69	4.33	125.83	121.00	3.84

Module ID	A			B			C			D			E			F			G			H		
Cell type	Single crystalline			Polycrystalline			Polycrystalline			Polycrystalline			2-a-Si			2-a-Si			CIS			CIS		
Glazing	Glass			Glass			ETFE			PVDF			Glass			Glass			Glass			Glass		
Insulated	Yes			Yes			Yes			Yes			No			Yes			No			Yes		
Month	Meas. (kW h)	Pred. (kW h)	% diff.	Meas. (kW h)	Pred. (kW h)	% diff.	Meas. (kW h)	Pred. (kW h)	% diff.	Meas. (kW h)	Pred. (kW h)	% diff.	Meas. (kW h)	Pred. (kW h)	% diff.	Meas. (kW h)	Pred. (kW h)	% diff.	Meas. (kW h)	Pred. (kW h)	% diff.	Meas. (kW h)	Pred. (kW h)	% diff.
January	10.62	10.62	−0.05	12.10	12.09	0.08	13.06	12.74	2.44	13.18	12.70	3.67	6.27	7.69	−22.62	6.24	7.51	−20.50	13.77	12.71	7.75	13.18	12.41	5.87
February	11.10	10.98	1.12	12.61	12.41	1.58	13.57	13.10	3.50	13.71	13.04	4.91	6.52	7.78	−19.34	6.52	7.62	−16.78	14.22	13.12	7.72	13.62	12.83	5.80
March	9.80	9.40	4.14	10.85	10.34	4.65	11.77	11.07	5.96	11.77	11.06	6.00	5.55	6.37	−14.94	5.60	6.27	−11.96	12.09	11.24	6.96	11.77	11.05	6.11
April	9.69	9.17	5.38	10.65	9.94	6.67	11.58	10.78	6.90	11.56	10.81	6.54	5.55	6.00	−8.15	5.58	5.92	−6.01	11.86	11.05	6.81	11.47	10.90	5.04
May	7.36	7.08	3.75	7.93	7.42	6.45	8.67	8.21	5.33	8.60	8.28	3.66	4.05	4.45	−9.68	4.11	4.40	−7.12	8.79	8.55	2.80	8.54	8.45	0.95
June	7.03	6.82	3.10	7.55	6.99	7.36	8.28	7.87	4.97	8.16	7.98	2.23	4.00	4.25	−6.25	4.01	4.21	−4.87	8.41	8.27	1.63	8.10	8.19	−1.18
July	7.36	7.25	1.52	7.97	7.52	5.64	8.74	8.42	3.64	8.64	8.52	1.39	4.30	4.58	−6.59	4.28	4.53	−5.90	8.97	8.82	1.68	8.60	8.73	−1.59
August	7.91	7.88	0.34	8.72	8.42	3.38	9.52	9.27	2.62	9.46	9.32	1.44	4.77	5.11	−7.02	4.73	5.04	−6.56	9.85	9.60	2.53	9.35	9.48	−1.40
September	9.68	9.65	0.33	10.96	10.67	2.68	11.86	11.51	3.02	11.91	11.50	3.42	6.00	6.52	−8.74	5.94	6.41	−7.97	12.45	11.71	5.97	11.67	11.52	1.34
October	6.98	6.90	1.18	7.93	7.64	3.66	8.54	8.20	3.96	8.58	8.21	4.41	4.22	4.77	−13.19	4.22	4.69	−11.01	8.94	8.34	6.77	8.43	8.19	2.93
November	7.89	7.84	0.60	8.96	8.82	1.61	9.67	9.34	3.32	9.72	9.32	4.14	4.56	5.56	−22.01	4.59	5.45	−18.70	10.14	9.39	7.35	9.69	9.20	5.12
December	9.20	9.26	−0.64	10.58	10.50	0.75	11.35	11.06	2.49	11.49	11.03	4.00	5.22	6.69	−28.08	5.27	6.54	−24.17	11.90	11.04	7.16	11.41	10.79	5.43
Total	104.62	102.84	1.70	116.81	112.77	3.46	126.62	121.58	3.98	126.79	121.77	3.96	61.00	69.77	−14.38	61.09	68.59	−12.27	131.39	123.84	5.74	125.83	121.73	3.26

Table 2.2: PV Model Efficiency Study - NIST [9]

2.5 Climatic Effects on PV Power Production

2.5.1 Temperature.

The effect temperature has on PV energy production is a well-documented and researched relationship. The variable with the largest relationship is the PV cell temperature, or the temperature of the system itself while operating [44]. Certain variables have been correlated as a function of the PV cell temperature including the ambient temperature, local wind speed, and solar radiation/irradiance [44]. Table 2.6 shows the various relationships between power, or similarly energy production, and temperature. Of the 28 functions listed, 15 of these list ambient temperature as having a correlation to power production. It can be concluded, therefore, that temperature, both operating and ambient, has a large relationship with the ability of a PV cell to produce power efficiently [12, 44].

2.5.2 Humidity.

Humidity, the percentage moisture present in the air at any one point in time, has been found to be a major concern to PV power production. In order for PV cells to work at their most efficient level, sunlight must to hit the cell in a direct or mostly direct manner; many PV cells are adjusted throughout the day and times of year to gather the most direct sunlight as possible. When there is a large presence of moisture in the air, the ability for sunlight to directly hit the cell becomes limited. As light passes through water droplets, three scenarios can happen. The light can be refracted, meaning the light will be redirected at a different angle. The light can be reflected, meaning the light is turned around back to its origin. Lastly, the light may be diffracted, or broken up into multiple angles different from the original. These three scenarios all can cause the irradiance of a PV cell to drop

Figure 2.6: PV Power Functions [44]

Table 3
PV array power as a function of temperature $P = \eta_c A G_T$.

Correlation	Comments	References
$P = \eta_{T_{ref}} A G_T (\tau\alpha)\left[1 - \beta_{ref}(T_P - T_{ref})\right]$	T_P = plate temperature, $\eta_{T_{ref}} = 0.118$ at 45 °C – air coll, $\eta_{T_{ref}} = 0.108$ at 28 °C – water coll	Hendrie (1979)
$P_{T_c} = \eta_{ref} A G_T K_f [1 + \alpha(T_c - 25)]$	$T_{ref} = 25$ °C, $\eta_{T_{ref}} = 0.13$, $\alpha = -0.004$ °C^{-1}, K_f factor for rest, frame installation, T_c in °C	Nishioka et al. (2003)
$P = \eta_e A G_T \tau_g p\left[1 - \beta_{ref}(T_c - 25)\right]$	p = packing factor, T_c in °C, τ_g = glazing transmissivity	Chow et al. (2006)
$P = \eta_{T_{ref}} A G_T [1 - 0.0045(T_c - 298.15)]$	$\eta_{T_{ref}} = 0.14$, T_c in K	Jie et al. (2007a)
$P = \eta_{T_{ref}} A G_T \tau_{pv} [1 - 0.0045(T_c - 25)]$	$\eta_{T_{ref}} = 0.14$, T_c in °C, τ_{pv} = pv cell glazing transmittance	Jie et al. (2007b)
$P = \eta_{T_{ref}} A G_T \left[1 - \beta_{ref}\left(T_c - T_{ref}\right) + \gamma \log_{10} G_T\right]$	$\beta_{ref} = 0.0044$ °C^{-1} for pc-Si, γ is usually taken as 0	Cristofari et al. (2006)
$P_T = P_{ref}\left[1 - \beta_{ref}(T - T_{ref})\right]$	$\beta_{ref} = 0.004$–0.006 °C^{-1}, T in °C, T_{ref} = reference temperature	Buresch (1983)
Same as above	$\beta_{ref} = 0.004$	Twidell and Weir (1986)
$P(T) = P(25)[1 - \gamma(T - 25)]$	$\gamma = 0.0053$ °C^{-1} for c-Si range: 0.004–0.006 °C^{-1}	Parretta et al. (1998)
$P_T = P_{25}[1 - 0.0026(T - 25)]$	a-Si, T in °C, power degrades to $0.82 P_{init}$	Yamawaki et al. (2001)
$P_T = P_{25} + \frac{dP}{dT}(T - 25)$	$\frac{dP}{dT} = -0.00407, -0.00535$, Si space cells, T in °C	Osterwald (1986)
$P(T) \approx G_T[\eta_0 - c(T - T_a)]$	η_0 = efficiency at T_a, c = temperature dependence factor	Bergene and Løvvik (1995)
$P_{max} = P_{max,ref}[1 - Df(T_c - 25)]$	Df = "deficiency factor" = 0.005 °C^{-1}	Al-Sabounchi (1998)
$P_{\max} = P_{\max,ref} \frac{G_T}{G_{T,ref}} \left[1 + \gamma\left(T_c - T_{ref}\right)\right]$	γ = temperature factor for power, $\gamma = -0.0035$ (range – 0.005 °C^{-1} to -0.003 °C^{-1}). T_c in °C	Menicucci and Fernandez (1988)
$P_{max} = P_{max,ref} \frac{G_T}{G_{T,ref}} [1 + \gamma(T_c - 25)]$	$\gamma = -0.0035$ (range – 0.005 °C^{-1} to -0.003 °C^{-1}) T_c in °C	Fuentes et al. (2007)
$P_{\max} = P_{\max,ref} \frac{G_T}{1000}\left[1 + \gamma\left(T_c - T_{ref}\right)\right]$	γ = temperature factor for power, $T_{ref} = 25$ °C, used in PVFORM	Marion (2002)
$P_{mp,T_r} = I_{mp,T}[1 - \alpha(T - T_r)]\left[V_{mp,T} - \beta V_{mp}^{STC}(T - T_r)\right]$	STC refers to ASTM standard conditions (1000 W/m^2, AMI = 1.5, $T_r = 25$ °C)	King et al. (1997)
$P_{max} = P_{max,ref} \frac{G_T}{G_{T_{ref}}} \left[1 + \alpha\left(T - T_{ref}\right)\right]\left[1 + \beta_{ref}\left(T - T_{ref}\right)\right] \left[1 + \delta(T) \ln\left(\frac{G_T}{G_{T_{ref}}}\right)\right]$	Adapted from the MER model[a]. Coefficient δ evaluated at actual conditions	Kroposki et al. (2000)
$P = P_0[1 + (\alpha - \beta_{ref})\Delta T]$	α: 0.0005 °C^{-1}, β: 0.005 °C^{-1}	Patel. (1999)
$P = (\alpha T_c + \beta) G_T$	α = temperature coefficient, β = calibration constant	Yang et al. (2000)
$P = -4.0 + 0.053 G_T + 0.13 T_c - 0.00026 G_T T_c$	MPPTracked 100 kWp system	Risser and Fuentes (1983)
$P = -0.4905 + 0.05089 G_T + 0.00753 T_c - 0.000289 G_T T_a$	MPPTracked 100 kWp system	Risser and Fuentes (1983)
$P_T = -8.6415 + 0.076128 G_T + 1.02318 \times G_T^2 + 0.20178 T - 4.9886 \times 10^{-3} T^2$	T is the panel temperature (K), too many significant figures!!!	Jie et al. (2002)
$P = G_T(b_1 + b_2 G_T + b_3 T_a + b_4 V_f)$	EPTC model, b_j regression coefficients, V_w^f wind speed 10 m above ground	Farmer (1992)
$P = c_1 + (c_2 + c_3 T_a) G_T + (c_4 + c_5 V_w) G_T^2$	c_j regression coefficients based on STC module tests[b]	Taylor (1986)
$P_{mp} = D_1 G_T + D_2 T_c + D_3 [\ln(G_T)]^m + D_4 T_c [\ln(G_T)]^m$	D_j (j = 1–4), m parameters[c]	Rosell and Ibáñez (2006)
$P = V_c I_c \left[1 - \frac{G_T - 500}{2.0 \times 10^{-4}} + \frac{C_{T_c}}{4 \times 10^4}(50 - T_c)^2\right]$	I_c = output current (A), V_c = output voltage (V), T_c in K, $C_{T_c} = 1$ if $T_c \leqslant 50$ °C or =3 if $T_c \geqslant 50$ °C	Furushima et al. (2006)
$P = A(0.128 G_T - 0.239 \times 10^{-3} T_a)$	p-Si, hybrid PV-fuel cells system G_T in kW/m^2, P in kW, T_a in °C	Zervas et al. (2007)
$P = P_{ref} G_T K_{pt} K_w K_e K_c$ with $K_{pt} = 1 + \alpha(T_c - 25)$	K_w, K_e, K_c loss coefficients due to mounting, dirt etc., AC conversion. Semitransparent PV	Wong et al. (2005)

Notes:

- Ref. Bücher et al. (1998): reports power temperature coefficients for various module types in the range [−0.0022/K to 0.0071/K], values around −0.002 referring to a-Si.
- Refs. Radziemska (2003) and Radziemska and Klugmann (2006): report power temperature coefficients −0.0065/K for c-Si.
- Ref. Fathi and Salem (2007): reports a dimensional expression for "power" – actually specific energy!
- Energy production correlation E_{out} {W hr} $= (\varepsilon_0 + \varepsilon_1 T_c)E$ {kW hr/m^2}, with $36.41 \leqslant \varepsilon_0 \leqslant 44.14$ and $-0.20 \leqslant \varepsilon_1 \leqslant -0.16$ is given in del Cueto (2001).
- Daily energy production (W h/day) is given by $E = A_1 H + A_2 H (T_{a,max})^{-2} + A_3 T_{a,max}$, with $T_{a,max}$ the maximum ambient temperature (°C), H the daily total insolation (W h/m^2/day) and A_j regression coefficients, according to the EMAT model (Meyer and van Dyk, 2000).
- Ref. Zhou et al. (2007) presents an expression for P_{max} based on BIPV data, which, for two states 0 and 1, is proportional to $(T_0/T_1)^\gamma$ with $\gamma = \frac{\ln(V_{oc_0}/V_{oc_1})}{\ln(T_1/T_0)}$.
- There are few equations with no explicit temperature dependence. Among them, the single regression yearly average form $P_{yr} = 0.1103 G_{T,yr}$ (Liu et al, 2004) and the nonlinear expression $P = c_1 G_T + c_2 G_T^2 + c_3 G_T \ln G_T$, with c_j regression coefficients, known as the ENRA model (Gianolli Rossi and Krebs, 1988), which over-predicts the PV performance.

[a] The V_{oc} and I_{sc} expressions have been combined as in Eq. (1).

[b] The regression equation shown combines the original equation for P and the analogous expression for T_c.

[c] For pc-Si, $D_1 = 0.000554$, $D_2 = -7.275 \times 10^{-5}$, $D_3 = 2.242 \times 10^{-5}$, $D_4 = -4.763 \times 10^{-8}$, $m = 7.0306$. Analogous sets are given for c-Si, a-Si, and thin film modules.

considerably as the percentage of moisture within the atmosphere increases [16, 34, 42]. Figure 2.7 shows the relationship between the irradiance and relative humidity.

Figure 2.7: Irradiance vs. Humidity Data [34]

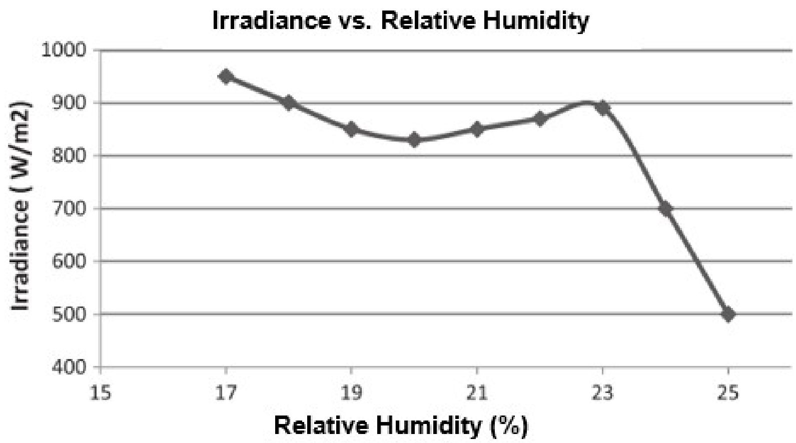

2.5.3 Air Mass.

Air mass, sometimes referenced as solar irradiance, is the relative path length of a direct solar beam through the atmosphere [42]. An air mass spectrum of 1.5 is used for models as can be seen in Figure 2.8a. This spectrum is important due to the ever changing angles at which these beams are captured. Furthermore, the effects of atmospheric conditions such as water vapor content and cloudiness of the region may further affect the ability to predict efficiency. The changing air mass figures due to these effects can be seen in Figure 2.8b. The conclusion of the study of air mass impact is that changing weather patterns accompanied with changing seasons will adversely affect the ability to predict efficiency of photovolatic systems [16, 42, 47].

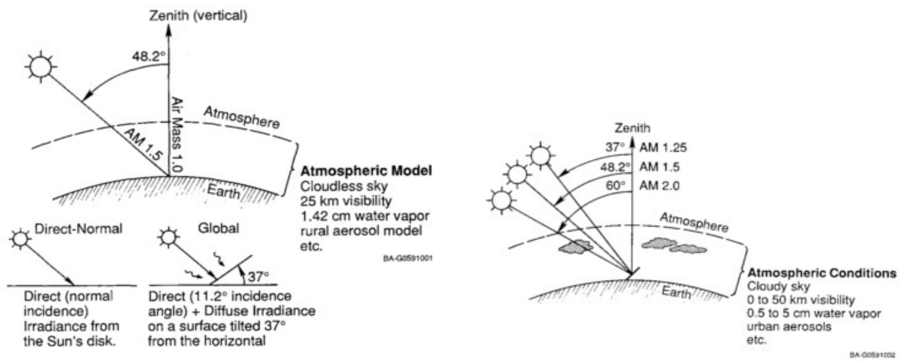

(a) Air Mass Spectrum [42]　　(b) Climate Effect on Air Mass [42]

Figure 2.8: Air Mass Effects

2.6 Dust Effects

A factor which does not receive much study is the effect of dust accumulation has upon a system. Dust accumulation is present in all climates with some being obviously more affected then others. The literature which studies these effects shows varied results with the overall conclusion being that dust negatively affects a system's ability to produce energy. Their results of energy production with dust accumulation ranged from as high as 50% to as low as 25% [24, 40]. These results can be seen in Figure 2.9. The conclusion which can be drawn is that depending on the climate region, dust accumulation can have a large negative impact on a photovoltaic system ability to function efficiently [24, 31, 40, 41].

2.7 Climate Classification

The major portion of this research involves analyzing the data gathered from the test systems in various climate regions to determine the most beneficial areas for Air Force photovoltaic investment. To further clarify, this study will aid the USAF in determining

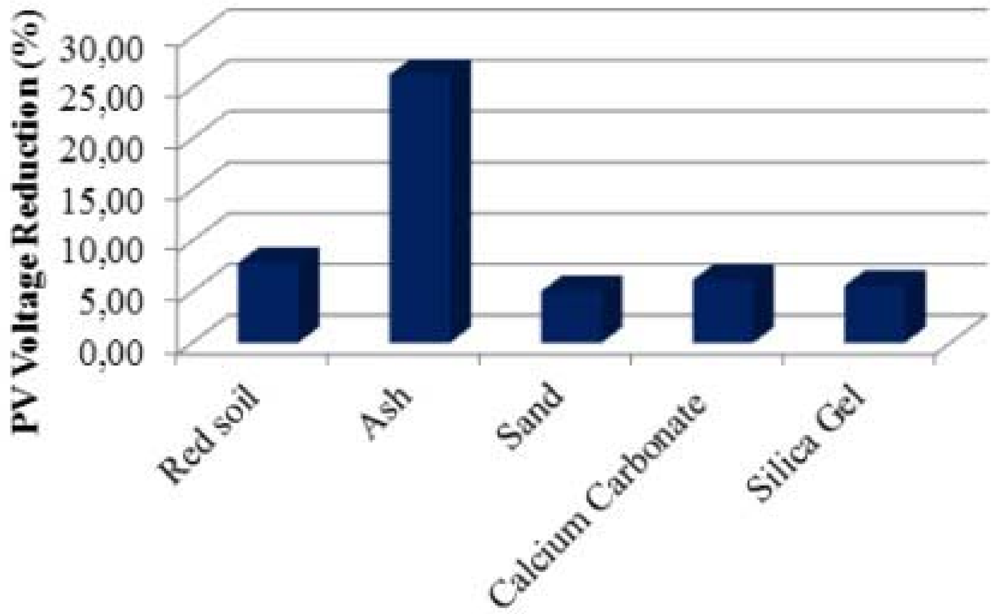

Figure 2.9: Dust Effects on Production [24]

where to invest in photovoltaic cells based upon the installation with the most efficient climate regions as realized in this study. It is, therefore, important to outline which climate classifications will be used for this study. The most frequently used system is the Köppen-Geiger climate classification system and will be used for this data analysis [6, 28].

The Köppen-Geiger climate classification system is built around the distinction of five vegetation groups. These five groups are the following: arid, warm temperate, snow, polar, and equatorial. Furthermore, the five groups are then divided into subgroups based upon the area's precipitation. The six precipitation groups are the following: desert, steppe, fully humid, summer dry, winter dry, and monsoonal. Lastly, the zones can be further delineated using a temperature classification. The eight groups used to distinguish temperature are the following: hot arid, cold arid, hot summer, warm summer, cool summer, extremely continental, polar frost, and polar tundra [5, 6, 23, 28, 30, 37]. Figure 2.10 shows the 30 total climate classifications based upon data gathered from 1951 to 2000 using a 0.5 degree latitude/longitude grid.

2.8 Case Studies

Multiple studies have been conducted in hopes of determining the effects of temperature and/or humidity on photovoltaic efficiency. Many of these studies have been conducted in Kuwait and surrounding countries in the Middle East region. Many of the countries still receive much of their energy production from oil and gas due to their large reserves. One of the common themes of these studies was analyzing how temperature and the presence of foreign materials, i.e., dust, affected the efficiency of the cells. One study found that the presence of dust on solar cells which were left uncleaned caused a 32% reduction in production [3]. However, all of the studies from this region collectively concluded that the region was well suited for investment due to the large capacity factors and overall photovoaltic efficiency [2, 3, 7, 11, 13, 20].

Other studies have been conducted in which Geographic Information Systems (GIS) are used to determine the best placement of photovolatic systems. One of the studies conducted in northern Africa used GIS data to determine where solar thermal plants could see the most benefit [8]. Solar thermal plants harness the solar energy to convert water to steam, which then turns a turbine to produce electricity. These studies provide insight into how alternative techniques, such as GIS, may be used to further determine photovolatic potential [8, 46, 52].

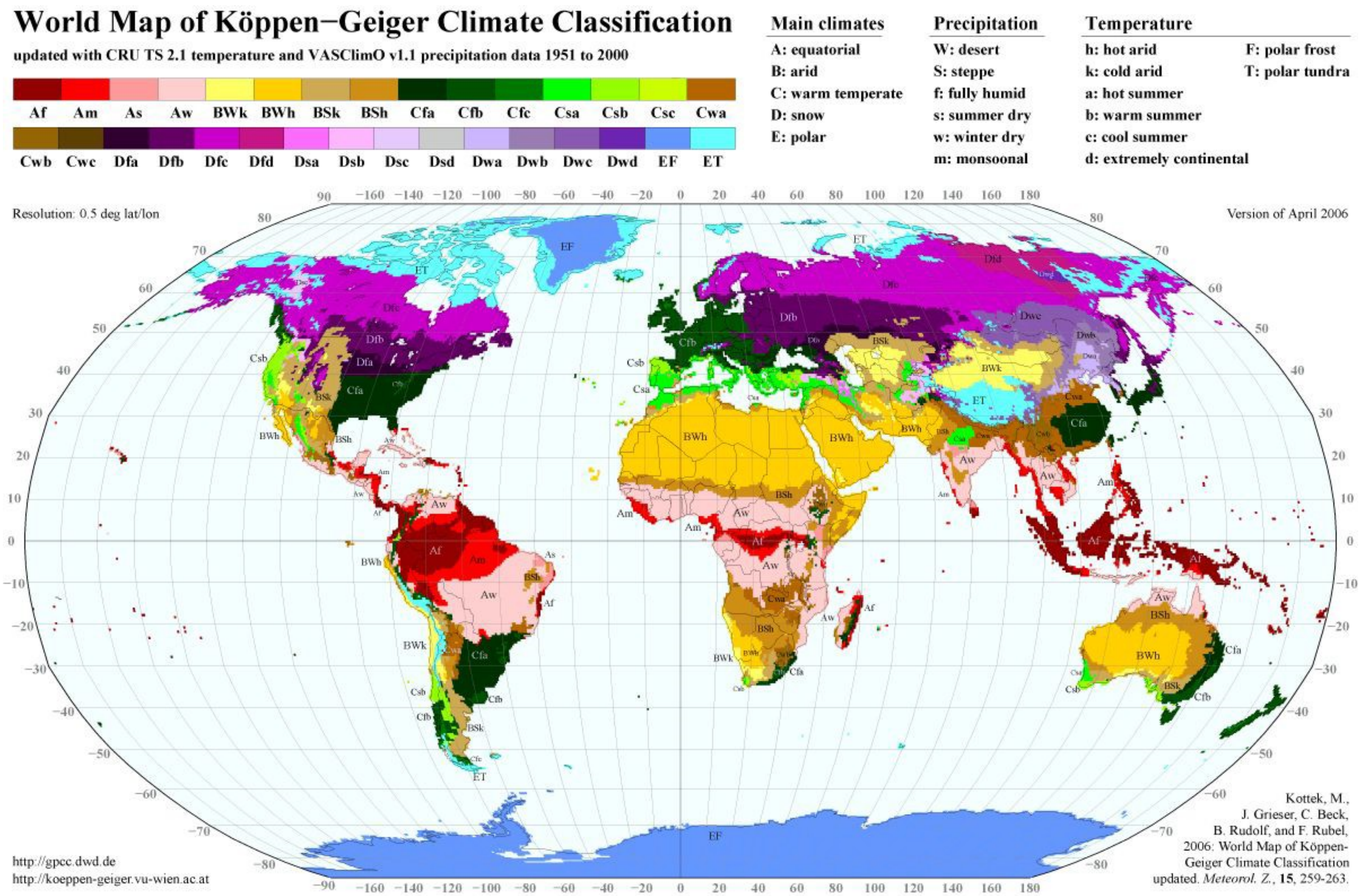

Figure 2.10: Koppen-Geiger Climate Classification World Map [28]

III. METHODOLOGY

The purpose of this chapter is to outline the methods and tools which are used to complete this research. The test system design is discussed as well as its various implementations in the field. Furthermore, the methods used to analyze the data collected are determined and discussed. Finally, the expected results from this analysis are considered.

3.1 Test System Design

The test systems used for this research were designed and manufactured at TecEdge Works located in Dayton, OH. The hardware and the associated software design was created in a prior research effort completed by Nussbaum and the Electrical Engineering Department located at the Air Force Institute of Technology (AFIT) [10]. The manufacturing of the test systems took place in the first quarter of 2017. Once complete, each test system was packaged and sent via official mail to the various locations for installation.

The two PV panels used for each test system were rated for 50 watts (poly-crystalline) and 25 watts (mono-crystalline). For the purposes of analysis, each panel's energy output is annotated per square foot. This was done to ensure easily comparable results when completing statistical analyses while adding variance in panel choices. Ideally, the same wattage panels would be used for this study for easier comparison. However, product availability at the time of purchase caused the different rated panels to be selected. The two panels are normalized based upon their rated wattage and overall size to produce comparable results. Silicone-based panels are used for this study due to the fact that they capture the largest market share, 70-90%, of available PV panels [36]. The justification of using the two different types of panels, mono-crystalline and poly-crystalline, is to ensure an appropriate amount of variance in panel construction is used to garner accurate results in the potentially multiple different makeups of existing and future solar arrays.

Each system's control unit consists of a satellite communication system, temperature/humidity probe, and computer. Readings from the PV panels and the probe will be taken at set intervals of fifteen minutes and stored upon a memory card within the test system. These readings include current and voltage for each panel, humidity, internal temperature of the control unit, and external ambient temperature. The fifteen minute readings for each panel are a collection of individual data points taken at ten second intervals for amperage and voltage. Each day, the control unit sends a health message via satellite showing daily averages of the measured data. The purpose of the daily messages is not to gather data, but rather to ensure the test system is working properly and to notify installation hosts of any potential issues. Each month the test system data is gathered by the location person of contact (POC). This POC electronically sends the Excel data file located upon the on-board memory card for analysis. The control units were outfitted with three light emitting diodes (LEDs): green, yellow, and red. These LEDs were installed to inform the participants of the systems functionality on a continual basis. The green LED was designed to flash whenever a reading was taking place. The yellow LED would stay lit to indicate the system was operating correctly. The red LED would light only if an error code was registered during the readings or if the system was found to be in fault at any times.

Each node, or panel, has a control box mounted to the backside of the frame to gather and send data of the node's performance to the main control box. The node chip diagram identifying major functions can be seen in Figure 3.1.

Figure 3.1: Node Chip Diagram [10]

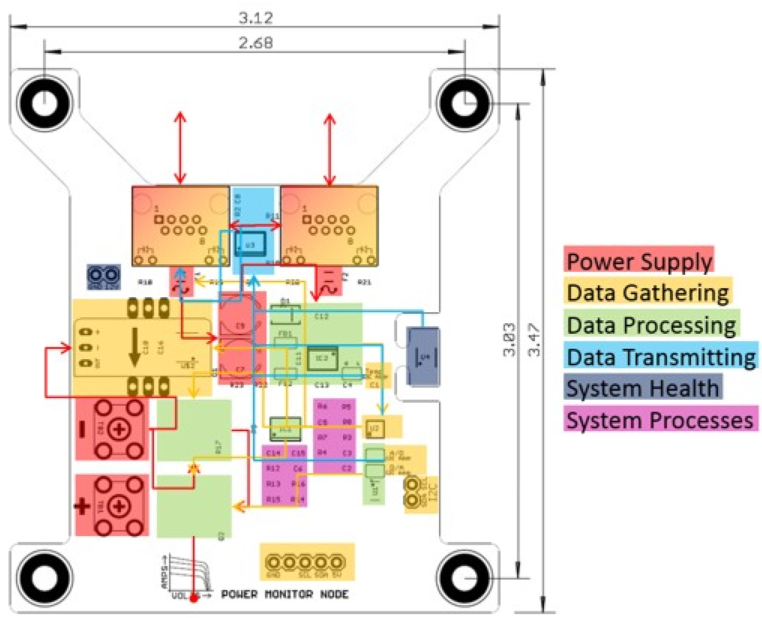

The base control unit gathers the performance data from the nodes and writes the data into an Excel sheet. The base chip is connected directly to a power source, either from a prime source, such as an outdoor power outlet, or an on-site battery. A diagram showing the major functions of the base chip can be seen in Figure 3.2. The chip runs using an on board Raspberry Pi™ computer. A Raspberry Pi™ is a small card which houses its own CPU, memory, and graphics card, making it a fully functioning computer [35, 48, 49]. The Raspberry Pi™ comes complete with Cat5 connections and additional memory storage in the form of MicroSD card ports. The size, benefits, and cost made this an ideal method to collect and consolidate the data. A MicroSD card formatted with the accompanying software package is inserted into the Rasberry Pi™.

Figure 3.2: Base Chip Diagram [10]

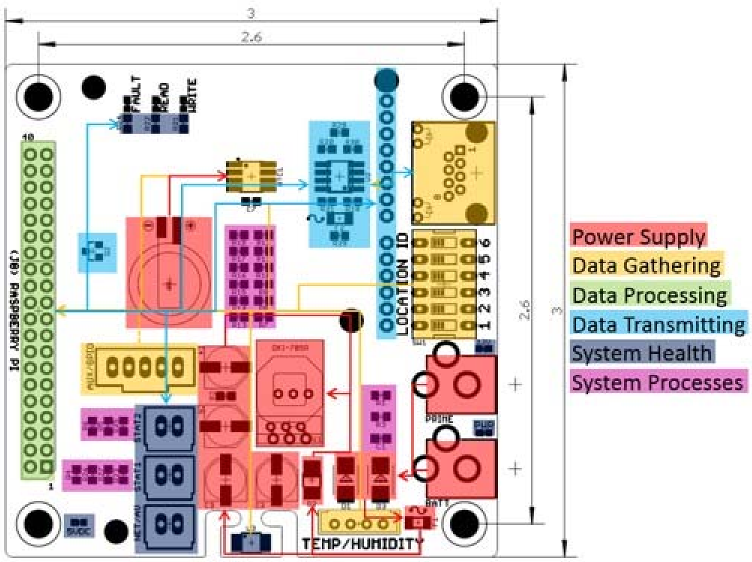

The installation hosts were given one month to install the test systems and report back any issues once the system was received. This was due to the unknown timeframe in which systems would be delivered to their test sites. Furthermore, questions with regards to setup and data retrieval were expected. Therefore, additional time needed to be allocated to ensure all participants were knowledgeable on setup and operation. The majority of test systems began collecting data in the June-July 2017 time frame. Beginning then, the locations sent back their collected data for analysis on the first day of each month. An example of installed test systems can be seen in Figure 3.3.

Figure 3.3: Installed Test Systems

3.2 Site Selection

The test sites were extracted from current Air Force installation data using JMP software [10]. This process starts with separating the 1,763 installation locations in bins based upon the latitude and longitude of each location. Once completed, an ANOVA analysis was conducted to determine an R Square value for each set. The histograms with the bin breakdown on coordinates for USAF installations can be seen in Figures 3.4a and 3.4b.

The analysis of the histograms provided distinct regions of the world in which to place these test systems. This, of course, limits the number of climates to be analyzed. However, for the purposes of determining the installations with the largest potential for energy production though, the analysis was sufficient. It provided 25 distinct regions in which Air Force installations are located, as can be seen in Figure 3.5. At this point,

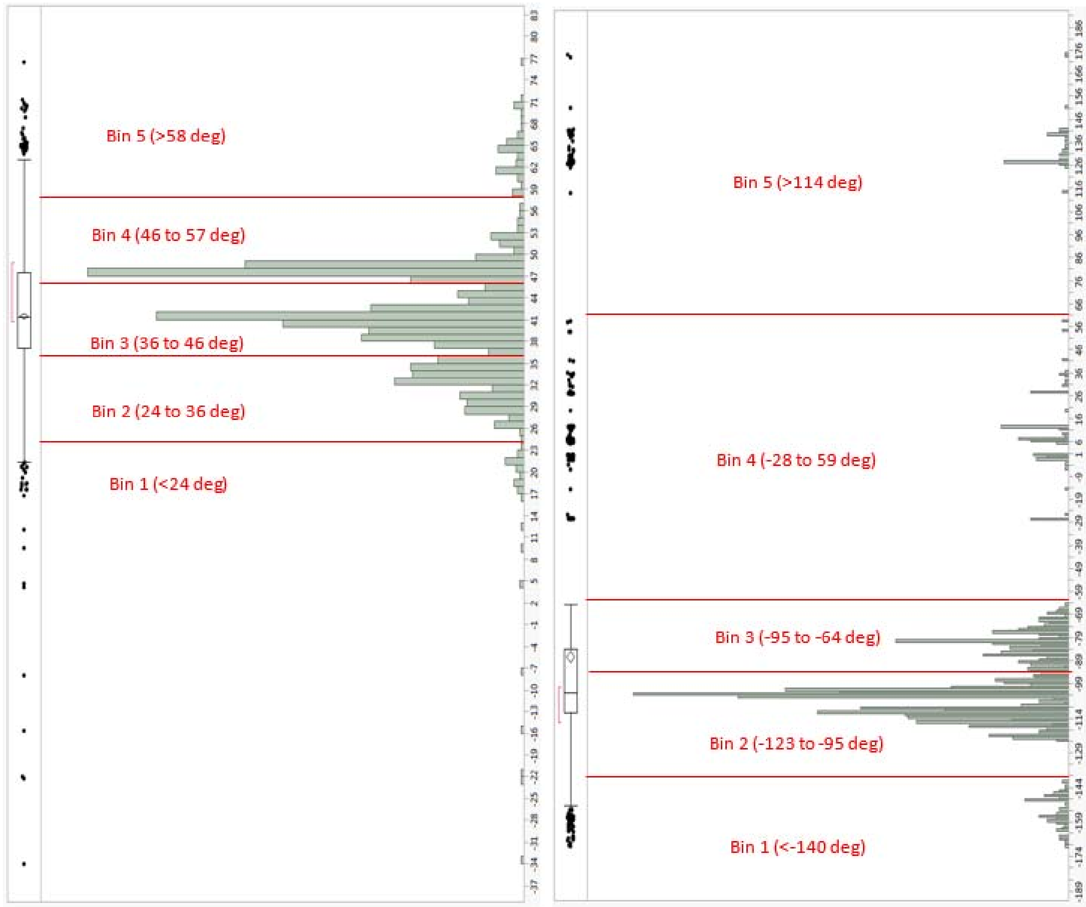

(a) Latitudes [10]

(b) Longitudes[10]

Figure 3.4: Histogram Breakdown of Air Force Installation Coordinates

the desired mean latitudes and longitudes of each region were compared to the actual installation locations from which the first round of installations were selected. This was not only based upon location, but on the hosts' availability and willingness to participate in the research. A sample of the selected test site locations can be seen in Table 3.1.

Figure 3.5: Installation Breakdown into 25 regions [10]

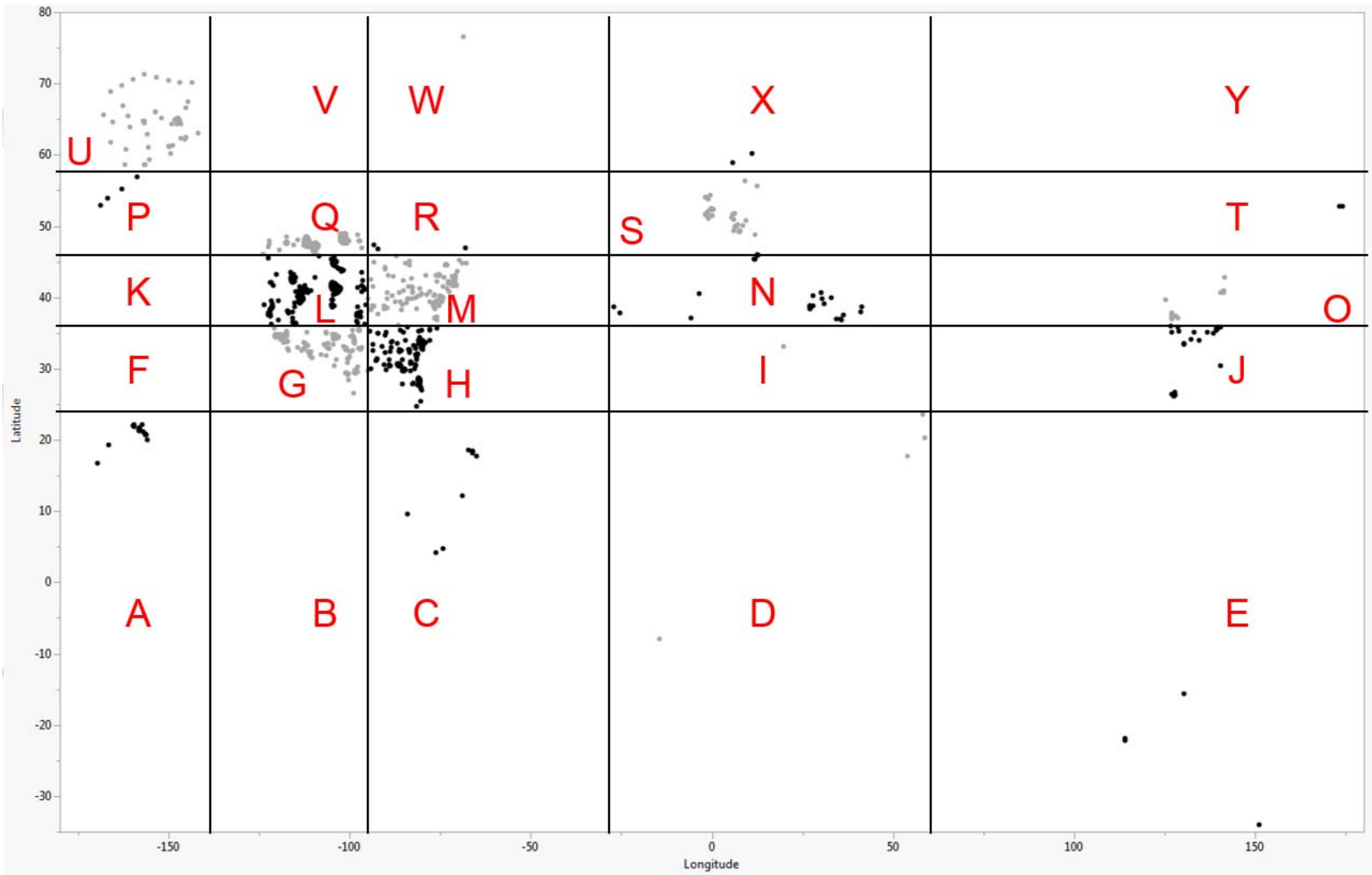

Region	Desired Lat	Desired Long	Selected Site Lat	Selected Site Long	Lat Delta	Long Delta
A	21.018	-158.882	20.882	-156.468	0.136	2.414
B	0.000	0.000	N/A	N/A	0.000	0.000
C	14.033	-70.077	12.183	-69.000	1.849	1.077
D	13.809	42.304	11.517	43.064	2.292	0.761
E	-23.401	127.464	-22.190	114.103	1.211	13.361
F	0.000	0.000	N/A	N/A	0.000	0.000
G	33.102	-106.165	32.919	-106.134	0.183	0.031
H	31.293	-83.625	31.167	-92.620	0.126	8.995
I	33.183	19.717	29.347	47.522	3.836	27.805
J	31.635	132.259	33.567	130.433	1.931	1.825
K	0.000	0.000	N/A	N/A	0.000	0.000
L	40.961	-108.217	40.943	-113.412	0.018	5.195
M	41.020	-79.920	40.670	-86.147	0.349	6.227
N	39.267	9.109	38.781	-27.145	0.486	36.255
O	38.396	130.630	39.650	125.333	1.254	5.297
P	54.787	-164.286	55.263	-162.807	0.476	1.479
Q	47.797	-107.344	47.795	-101.298	0.002	6.046
R	46.924	-89.278	46.934	-67.913	0.011	21.365
S	50.048	5.848	50.026	6.799	0.022	0.951
T	52.776	173.643	52.720	174.106	0.057	0.464
U	64.024	-152.668	64.291	-149.187	0.267	3.481
V	0.000	0.000	N/A	N/A	0.000	0.000
W	76.531	-68.703	76.531	-68.703	0.000	0.000
X	59.375	7.517	58.963	5.733	0.411	1.784
Y	0.000	0.000	N/A	N/A		

Table 3.1: Desired versus Actual Physical Locations [10]

The additional seventeen test sites were chosen using a Pareto analysis and the Köppen-Geiger Classification system, to ensure the largest breadth of climate types as possible were represented as well as acknowledging installations and climate types which were outliers in the analysis. The Pareto analysis, revealed that the USAF had installations in 23 of the 30 climate classifications. Of those 23, 15 climate types had less than 1% of USAF installations located within them. The Pareto analysis was able to provide guidance on where additional systems were to be sent based upon these percentages. Due to budgetary concerns, only a certain number of test systems could be manufactured and

Figure 3.6: Final Test System Locations

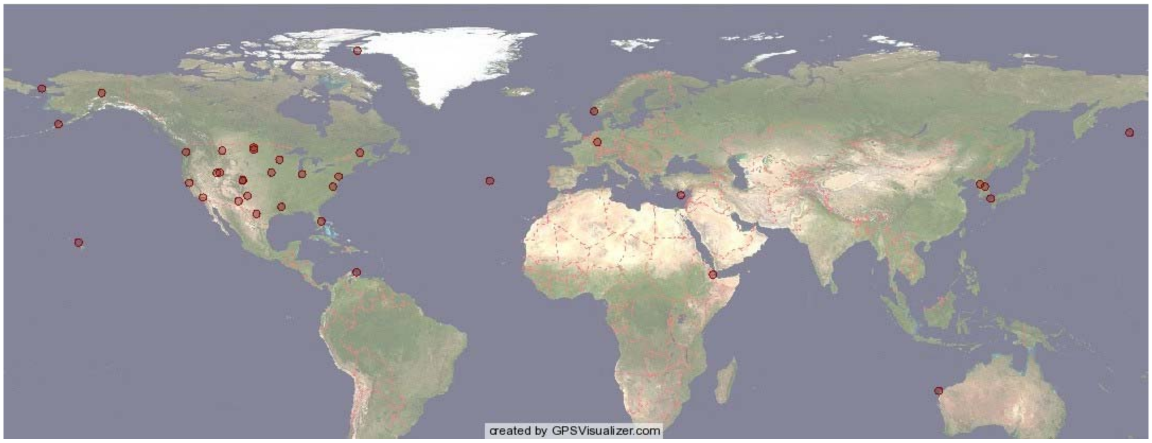

shipped, so it was important to ensure the research could provide usable data for the USAF and DoD as a whole. The results from this final round of analysis and decision making can be seen in Table 3.2. A map showing the final locations of all test systems can be seen in Figure 3.6.

Each of the chosen installations were contacted via email through their respective energy offices. Energy office employees were the ideal choice to be the study's POCs because the study wanted to ensure that the participants which would be handling the data collection had some background information and knowledge on the topic. If the energy office was unable to participate or the installation had no energy specific entity, the study was assigned a POC under the best judgment of the commanding officials at the site location. After initial site selection, one installation chose not to participate after undergoing a change of command. A replacement location was chosen based upon the next closest available site to the desired location coordinates.

Köppen-Geiger Climate Classifications	Total Installation Count	Installation Pareto Analysis	Total Test Site Count	Test Site Pareto Analysis
Arid/Steppe/Cold Arid	613	34.77	6.00	16.67
Warm Temperate/Fully Humid/Hot Summer	340	19.29	4.00	11.11
Snow/Fully Humid/Warm Summer	307	17.41	4.00	11.11
Warm Temperate/Fully Humid/Warm Summer	97	5.50	2.00	5.56
Warm Temperate/Summer Dry/Warm Summer	82	4.65	3.00	8.33
Snow/Fully Humid/Hot Summer	55	3.12	3.00	8.33
Snow/Fully Humid/Cool Summer	54	3.06	2.00	5.56
Warm Temperate/Summer Dry/Hot Summer	49	2.78	2.00	5.56
Arid/Desert/Cold Arid	17	0.96	0.00	0.00
Arid/Steppe/Hot Arid	16	0.91	2.00	5.56
Polar//Polar Tundra	12	0.68	2.00	5.56
Arid/Desert/Hot Arid	11	0.62	2.00	5.56
Snow/Winter Dry/Hot Summer	11	0.62	2.00	5.56
/Fully Humid/	10	0.57	2.00	5.56
/Summer Dry/	10	0.57	0.00	0.00
Snow/Summer Dry/Warm Summer	7	0.40	0.00	0.00
/Monsoonal/	5	0.28	0.00	0.00
Snow/Summer Dry/Cool Summer	3	0.17	0.00	0.00
/Winter Dry/	3	0.17	0.00	0.00
Warm Temperate/Winter Dry/Hot Summer	2	0.11	0.00	0.00
Snow/Summer Dry/Hot Summer	1	0.06	0.00	0.00
Snow/Winter Dry/Warm Summer	1	0.06	0.00	0.00
Warm Temperate/Fully Humid/Cool Summer	1	0.06	1.00	2.78

Table 3.2: Pareto Analysis of All Installations versus Final Test Site Selection [10]

3.3 Construction/Assembly

The manufacturing, assembly, and shipping of the test systems occurred at TecEdge Works located in Dayton, OH. The manufacturing occurred over a period of five months in late 2016 and early 2017. The materials were both off-the-shelf as well as some custom designed. Assembly proceeded over the following months as materials became available. A major portion of the assembly process was conducted while hosting a Science, Technology, Engineering, and Math (STEM) event for high school students from a local school.

After the major assembly was completed, each system was tested for functionality. All added penetrations were sealed with either epoxy or a silicone adhesive. The final step was the application of labels to give instructions and warnings for the host installations. A copy of this label can be seen in Figure 3.7.

Figure 3.7: Test System Instruction Label [10]

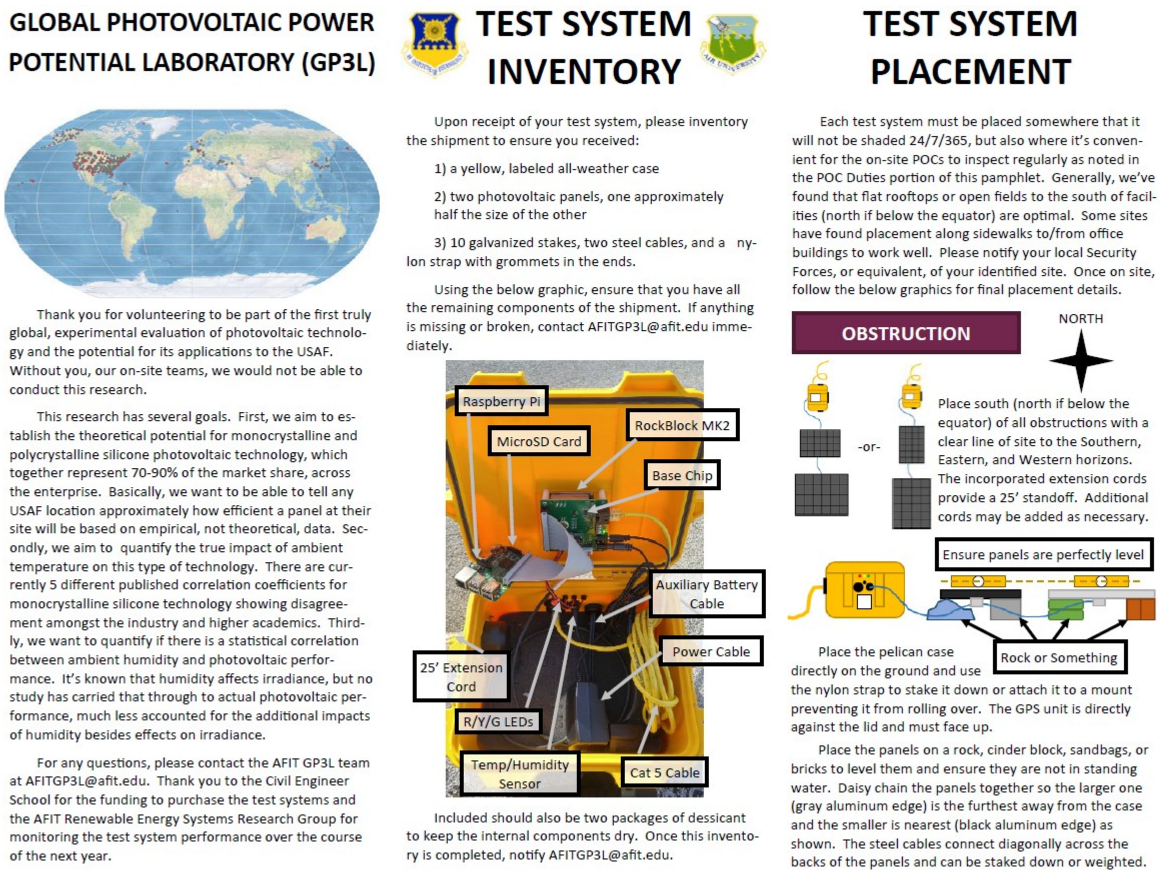

GLOBAL PHOTOVOLTAIC POWER POTENTIAL LABORATORY (GP3L)

Thank you for volunteering to be part of the first truly global, experimental evaluation of photovoltaic technology and the potential for its applications to the USAF. Without you, our on-site teams, we would not be able to conduct this research.

This research has several goals. First, we aim to establish the theoretical potential for monocrystalline and polycrystalline silicone photovoltaic technology, which together represent 70-90% of the market share, across the enterprise. Basically, we want to be able to tell any USAF location approximately how efficient a panel at their site will be based on empirical, not theoretical, data. Secondly, we aim to quantify the true impact of ambient temperature on this type of technology. There are currently 5 different published correlation coefficients for monocrystalline silicone technology showing disagreement amongst the industry and higher academics. Thirdly, we want to quantify if there is a statistical correlation between ambient humidity and photovoltaic performance. It's known that humidity affects irradiance, but no study has carried that through to actual photovoltaic performance, much less accounted for the additional impacts of humidity besides effects on irradiance.

For any questions, please contact the AFIT GP3L team at AFITGP3L@afit.edu. Thank you to the Civil Engineer School for the funding to purchase the test systems and the AFIT Renewable Energy Systems Research Group for monitoring the test system performance over the course of the next year.

TEST SYSTEM INVENTORY

Upon receipt of your test system, please inventory the shipment to ensure you received:

1) a yellow, labeled all-weather case

2) two photovoltaic panels, one approximately half the size of the other

3) 10 galvanized stakes, two steel cables, and a nylon strap with grommets in the ends.

Using the below graphic, ensure that you have all the remaining components of the shipment. If anything is missing or broken, contact AFITGP3L@afit.edu immediately.

Included should also be two packages of dessicant to keep the internal components dry. Once this inventory is completed, notify AFITGP3L@afit.edu.

TEST SYSTEM PLACEMENT

Each test system must be placed somewhere that it will not be shaded 24/7/365, but also where it's convenient for the on-site POCs to inspect regularly as noted in the POC Duties portion of this pamphlet. Generally, we've found that flat rooftops or open fields to the south of facilities (north if below the equator) are optimal. Some sites have found placement along sidewalks to/from office buildings to work well. Please notify your local Security Forces, or equivalent, of your identified site. Once on site, follow the below graphics for final placement details.

Place south (north if below the equator) of all obstructions with a clear line of site to the Southern, Eastern, and Western horizons. The incorporated extension cords provide a 25' standoff. Additional cords may be added as necessary.

Place the pelican case directly on the ground and use the nylon strap to stake it down or attach it to a mount preventing it from rolling over. The GPS unit is directly against the lid and must face up.

Place the panels on a rock, cinder block, sandbags, or bricks to level them and ensure they are not in standing water. Daisy chain the panels together so the larger one (gray aluminum edge) is the furthest away from the case and the smaller is nearest (black aluminum edge) as shown. The steel cables connect diagonally across the backs of the panels and can be staked down or weighted.

3.4 Test System Setup

At every test site, each panel will lay flat (zero degree tilt angle). Each test site location was individually responsible for the installation of the test systems. The lack of on-site assistance for the installation process created the need for a simple system setup. Additionally, the statistical analysis portion of the research may have been negatively affected by the wide range of tilt angle positions that were not able to be monitored or confirmed. It was decided for conformity and ease of system setup that each installation would place their systems in a flat position. Additionally, having zero degree tilt angles allows for data to be used on future solar pavement applications.

Once the test systems were received at each location, the participants were instructed to install them following a specific list of directions. These directions are referenced in Figure 3.7, the control box system label. The recommendation to the installations was to have the systems installed on a rooftop or an open field. However, the installations were given the freedom to choose on where the system would ultimately be placed. The participants were instructed that the systems be placed where they would have full sun the entire day. Furthermore, the systems were to be in a location with a clear view of the southern, eastern, and western horizons. This was to ensure that each panel received the maximum amount of sunlight per day. The installations were provided with stakes and tie-downs to ensure the system's stability. Some installations constructed housing units for the panels, while others simply placed the systems onto wooden pallets. Each location complied with the directed installation constructions.

3.5 Analysis

The data gathered from the test systems is consolidated into master files for each location. Because of the large number of data points gathered from each location, consolidation is necessary. Each data row, which consists of 64 voltage and 64 amperage measurements taken during the fifteen minute intervals, is used to find the accompanying power measurements. The power measurements are found by coupling each voltage and amperage measurement taken at set time intervals. The max power measurement is then found by taking the largest power calculated from the 64 data points. The single fifteen minute max power data point is then transcribed into a separate data file. This process repeats for each PV panel. The consolidated data file will also include all external measurements, such as temperature and humidity, with the accompanying time, location, and climate classifications. Once a satisfactory number of months have been recorded, the monthly power averages for each site, normalized for PV size and wattage, are calculated.

The PV panels must be normalized is to have comparable results for analysis. Each panel, being different sizes, will be converted to a per square foot measurement. The wattage normalization will begin with comparing the rated power capacity of the mono-crystalline panel to the poly-crystalline panel. The efficiency difference in the rated wattage is 25 watts/50 watts, or 50%. This means that the mono-crystalline panel has the capacity to produce 50% of what the poly-crystalline panel is rated. To normalize this data, the difference of 50% will be multiplied by and added to the mono-crystalline output. This will produce an output in which both panels can be analyzed as 50 watt rated.

When the monthly power averages for each location are determined, this data is statistically analyzed to determine which climate regions performed the best and the most consistently. This analysis will be completed by performing a linear regression for each main climate region based upon the data gathered. Once completed, each climate region will be analyzed via an ANOVA analysis to determine if the changes in temperature and precipitation classifications contribute to any statistically significant differences. These results will be able to provide greater insight on which USAF installation climate regions could see the most benefit from the implementation of PV technology.

Once the most viable climate region classifications have been identified, the data will be used to create a baseline model for expected energy output. This can be used in life cycle cost analyses to determine the payoff terms for investment into photovoltaic systems.

IV. DATACOLLECTION/ANALYSIS

4.1 Data Collection

4.1.1 Problems Encountered.

All test systems shipped to their respective locations in May of 2017. During the process of shipment and delivery, certain complications occurred. Two test sites received cracked panels, thus requiring the procurement of additional panels and their subsequent shipment. This setback, of course, delayed the installation of those systems.

An additional and unfortunate setback for the study was the realization that due to the high turnover rate at military installations, many of the positive relationships, formed under the excitement for participation in this study, were no longer in place when panels finally arrived. This became apparent when of the installations with which we initially had agreements in place, became hard to contact. This resulted in some systems taking months to be set up and others not at all. These setbacks are unfortunate. However, the large amount of data which has been and will continue to be gathered will still provide important insights. Refer to Table 4.1a to see the installed locations in bold.

As stated previously, the systems were sent and received in May 2017. Due to the time which was lost, due to systems not being promptly installed, data gaps emerged. Additionally, hardware and software issues surfaced. One intermittent problem identified at a few installations was that only one of the two panels recorded measurements. The error was linked to faulty CAT5 cables, which the hosts were then instructed to change if possible. Often, these problems were not realized until the end of each month during data

Region	Site	Main	Precip	Temp
C	Site 1:	Arid	Steppe	Hot Arid
D	Site 1:	Warm Temperate	Summer Dry	Warm Summer
E	Site 1:	Arid	Desert	Hot Arid
G	Site 1:	Arid	Steppe	Cold Arid
G	Site 4:	Warm Temperate	Summer Dry	Hot Summer
H	Site 1:	Warm Temperate	Fully Humid	Hot Summer
I	Site 1:	Arid	Desert	Hot Arid
L	Site 1:	Arid	Steppe	Cold Arid
L	Site 2:	Snow	Fully Humid	Hot Summer
L	Site 3:	Warm Temperate	Summer Dry	Hot Summer
L	Site 4:	Arid	Steppe	Cold Arid
L	Site 5:	Arid	Steppe	Cold Arid
L	Site 6:	Snow	Fully Humid	Warm Summer
M	Site 1:	Snow	Fully Humid	Hot Summer
M	Site 2:	Warm Temperate	Fully Humid	Hot Summer
M	Site 4:	Snow	Fully Humid	Hot Summer
N	Site 1:	Warm Temperate	Summer Dry	Warm Summer
O	Site 1:	Snow	Winter Dry	Hot Summer
Q	Site 2:	Warm Temperate	Summer Dry	Warm Summer
Q	Site 5:	Arid	Steppe	Cold Arid
R	Site 1:	Snow	Fully Humid	Warm Summer
S	Site 1:	Warm Temperate	Fully Humid	Warm Summer
A	Site 1:	Equatorial	Fully Humid	
G	Site 2:	Arid	Steppe	Hot Arid
G	Site 3:	Arid	Steppe	Cold Arid
H	Site 2:	Warm Temperate	Fully Humid	Warm Summer
J	Site 1:	Warm Temperate	Fully Humid	Hot Summer
M	Site 3:	Warm Temperate	Fully Humid	Hot Summer
O	Site 3:	Snow	Winter Dry	Hot Summer
P	Site 1:	Warm Temperate	Fully Humid	Cool Summer
Q	Site 1:	Snow	Fully Humid	Warm Summer
Q	Site 4:	Snow	Fully Humid	Warm Summer
T	Site 1:	Snow	Fully Humid	Cool Summer
U	Site 1:	Snow	Fully Humid	Cool Summer
U	Site 2:	Polar		Polar Tundra
W	Site 1:	Polar		Polar Tundra
X	Site 1:	Warm Temperate	Fully Humid	Warm Summer

Table 4.1: Installed/Missing Locations

(a) Installed locations in Bold

collection. The reason for the delay in recognizing many of these errors was due to the inaccurate and unreliable daily health messages, which were originally designed to be sent by satellite via the on board RockBlock. This was quickly realized to be ineffective and a waste of resources and the health message system was quickly abandoned.

4.1.2 Data Collection/Cleaning.

The hosts delivered their data electronically at the end of each month. The data was either emailed or uploaded to a shared drive. This was found to be the easiest and most efficient method to transmit data back to AFIT. Once the data had been gathered from all participating installations, the Excel sheets were consolidated and analyzed to give power outputs for each of the panels. Once completed, the cleaned data was transferred to a master file which encompassed all relevant data gathered from each installation. This process ensured that the analysis would be free from errors and omissions and informed hosts if problems had occurred which were not initially realized.

4.1.3 Data Analysis.

The data analysis was completed using JMP statistical software. The first step was to view the distributions of each panel's power output/SF. One initial observation is many data points were at or near zero. This was expected as the panels were not producing power during night hours. See Figure 4.1 for the box plot distributions including the described outliers.

Figure 4.1: Data Distribution Box Plots

(a) 25 Watt Mono-crystalline (b) 50 Watt Poly-crystalline

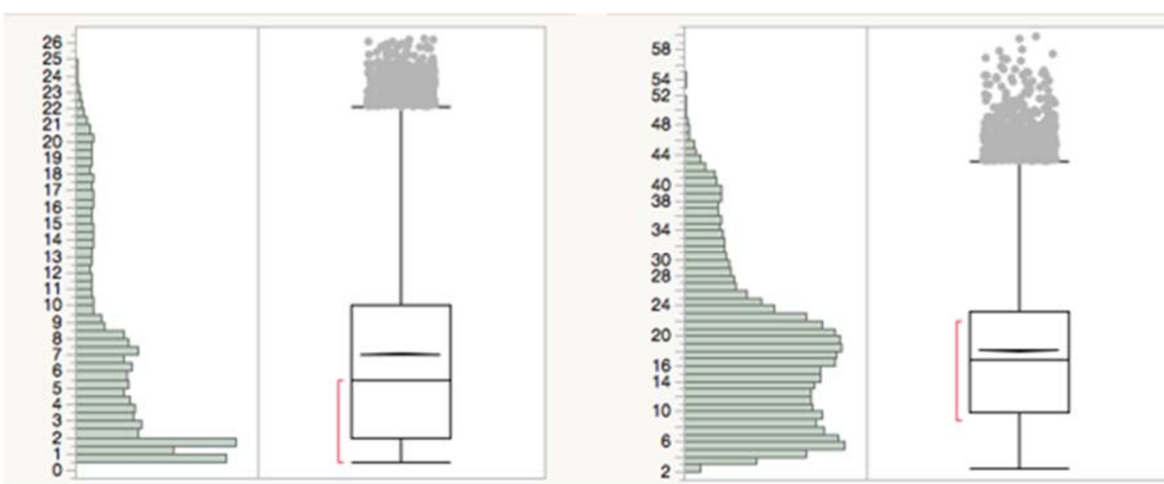

After the outliers at or near zero were excluded from the data set, the data characteristics were then tabulated. This was accomplished by analyzing the mean of both panels by installation location and by each climate classification. Given the large amount of data, the means were divided monthly. With a full year worth of data, this analysis would be better associated with seasons rather than months. The analysis was then shown graphically to aid in interpretation. Refer to Tables 4.2 and 4.3 for the tabulated means.

Figure 4.2 shows the normalized monthly power averages for both panels. This was completed by finding the efficiency of the mono-crystalline panels compared to the poly-crystalline panels at the same site. The mono-crystalline power measurements were normalized based upon the size of the panels used and the rated wattage. Size normalization was completed by analyzing the power measurements per square foot. Wattage normalization was accomplished by converting the 25 watt rated mono-crystalline panel data to what would be produced if it were rated 50 watts.

The next portion of the analysis involved determining if the interaction between the climate sub classifications had any effect on power output. The three sub classifications paired together were main climate, precipitation, and temperature. The interactions analyzed were main-precipitation and precipitation-temperature. The results of the analysis of variance (ANOVA) showed both interactions to be significant. These tests will be rerun annually when a more comprehensive data set is available for a full factorial analysis. The preliminary results of the power production of these climate regions can be seen in Figures 4.3 and 4.4 for the poly-crystalline panels. The analysis of the mono-crystalline panel's climate region interactions produced similar results.

Figure 4.2: Normalized Monthly 50 Watt Power Averages - Monocrystalline vs. Polycrystalline

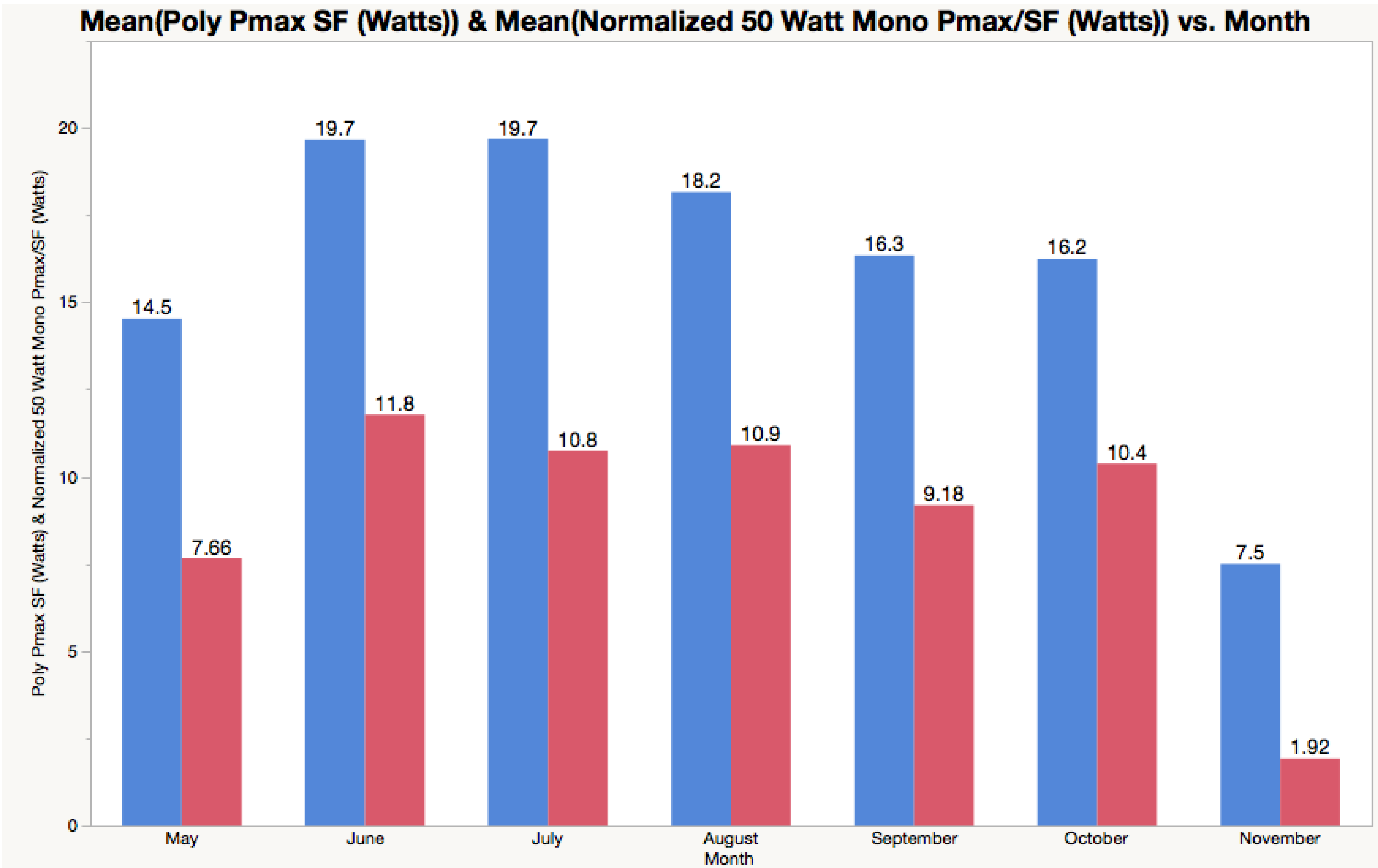

Location	May	June	July	August	September	October	November
	Mean	Mean	Mean	Mean	Mean	Mean	Mean
	Mono Pmax SF	Mono Pmax SF	Mono Pmax SF	Mono Pmax SF	Mono Pmax SF	Mono Pmax SF	Mono Pmax SF
Camp Murray	.	12.09	12.82	11.26	8.977	7.543	.
Camp Red Cloud	.	3.829	4.343	.	.	.	.
Chabelley	.	12.8	.	.	.	.	.
Curacao	.	.	.	3.978	5.969	2.449	.
DFAS Annex	.	.	.	3.157	2.519	1.977	1.277
Grissom	.	.	.	3.987	2.991	1.027	.
Grosslittgen, Spangdahlem	.	.	10.23	9.112	7.602	5.07	.
Hill Weber	.	.	.	3.987	2.991	1.027	.
Holloman	.	.	.	.	5.602	.	.
Lajes	.	.	.	11.1	10.66	9.183	.
Langley	.	4.026	3.663	3.42	2.12	2.4	.
Learmonth Solar Obs	.	.	.	.	4.543	.	.
Malmstrom	.	.	14.03	11.99	10.31	7.733	.
March AFB	.	.	4.595	5.303	2.774	.	.
Minn ANG	5.11	4.3	3.967	.	2.211	.	.
Offutt	.	4.613	3.012	3.296	5.481	.	.
Peterson	.	12.05	3.818	3.427	4.891	.	.
RAF Akrotiri	.	4.647	0.536	.	.	.	.
Travis	.	14.83	14.55	13.17	.	10.59	.
USAFA	.	4.331	2.197	1.668	1.679	.	.
WPAFB	.	.	.	8.911	8.336	7.104	.
Main							
Arid	.	5.526	3.154	6.469	4.605	7.501	.
Snow	5.11	4.371	4.067	3.652	2.737	1.94	1.277
Warm Temperate	.	12.18	10.43	9.504	8.562	7.498	.
Precip							
Desert	.	4.647	0.536	.	4.543	.	.
Fully Humid	5.11	4.38	5.771	5.308	5.502	4.004	1.277
Steppe	.	6.376	4.441	6.469	4.651	7.501	.
Summer Dry	.	13.44	11.3	10.22	9.289	9.362	.
Winter Dry	.	3.829	4.343	.	.	.	.
Temp							
Cold Arid	.	6.376	4.441	7.062	4.406	7.733	.
Hot Arid	.	4.647	0.536	3.978	4.791	2.449	.
Hot Summer	5.11	7.237	7.876	7.192	6.223	7.503	.
Warm Summer	.	12.57	12.09	7.779	7.187	6.152	1.277

Table 4.2: Monocrystalline Monthly Power/SF Averages

	Month						
	May	June	July	August	September	October	November
	Mean	Mean	Mean	Mean	Mean	Mean	Mean
Location	**Poly Pmax SF**	**Poly Pmax SF**	**Poly Pmax SF**	**Poly Pmax SF**	**Poly Pmax SF**	**Poly Pmax SF**	**Poly Pmax SF**
Camp Murray	.	25.59	26.57	23.45	19.54	17.6	.
Camp Red Cloud	.	12.17	15.4	.	.	.	.
Chabelley	.	24.21	.	.	.	.	.
Curacao	.	.	.	16.59	24.96	25.3	.
DFAS Annex	.	.	.	12.21	10.96	9.834	7.505
Grissom	.	.	.	14.06	15.75	18.61	.
Grosslittgen, Spangdahlem	.	.	21.98	20	16.77	12.62	.
Hill Weber	.	.	.	14.06	15.75	18.61	.
Holloman	.	.	.	.	16.37	.	.
Lajes	.	.	.	22.22	21	18.01	.
Langley	.	15.57	16.46	15.45	11.78	12.98	.
Learmonth Solar Obs	.	.	.	.	16.25	.	.
Malmstrom	.	.	28.95	24.92	21.76	17.7	.
March AFB	.	.	14.76	14.19	17.94	.	.
Minn ANG	14.52	14.1	14.27	.	22.4	.	.
Offutt	.	15.57	13.04	14.58	23.85	.	.
Peterson	.	24.65	14.37	16.62	24.06	.	.
RAF Akrotiri	.	17.28	15.97	.	.	.	.
Travis	.	30.62	29.82	26.97	.	21.59	.
USAFA	.	13.88	11.78	11.38	10.02	.	.
WPAFB	.	.	.	15.75	14.11	12.02	.
Main							
Arid	.	17.02	15.42	18.35	15.98	18.03	.
Snow	14.52	14.47	14.59	13.63	13.19	10.18	7.505
Warm Temperate	.	25.44	23.57	20.47	17.82	16.74	.
Precip							
Desert	.	17.28	15.97	.	16.25	.	.
Fully Humid	14.52	14.96	17.17	15.16	14.38	11.95	7.505
Steppe	.	16.77	15.15	18.35	15.77	18.03	.
Summer Dry	.	26.96	24.67	21.8	20.05	19.54	.
Winter Dry	.	12.17	15.4	.	.	.	.
Temp							
Cold Arid	.	16.77	15.15	18.77	14.07	17.7	.
Hot Arid	.	17.28	15.97	16.59	17.76	25.3	.
Hot Summer	14.52	19.09	20.26	17.71	14.78	17	.
Warm Summer	.	24.67	25.27	18.52	17.15	14.9	7.505

Table 4.3: Polycrystalline Monthly Power/SF Averages

Figure 4.3: Poly - Main/Precipitation Interactions

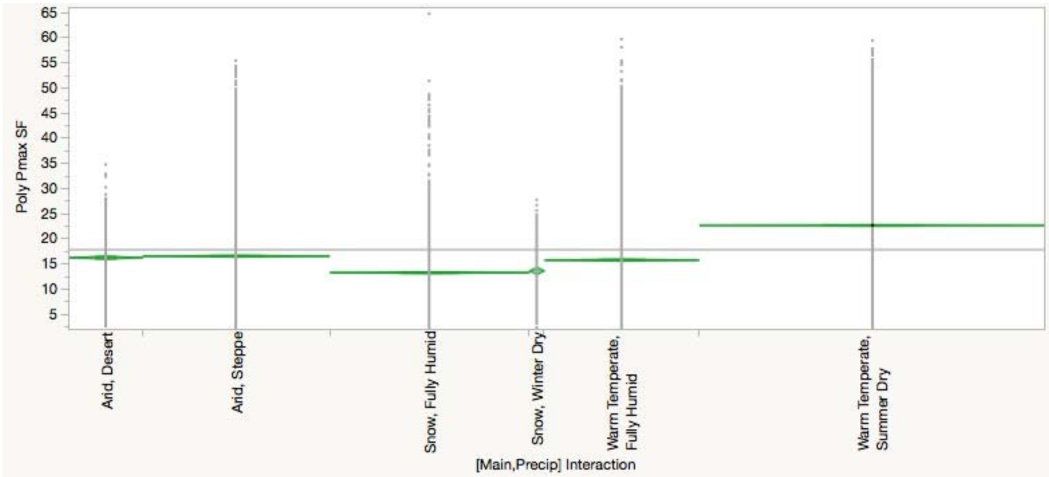

Figure 4.4: Poly - Precipitation/Temperature Interactions

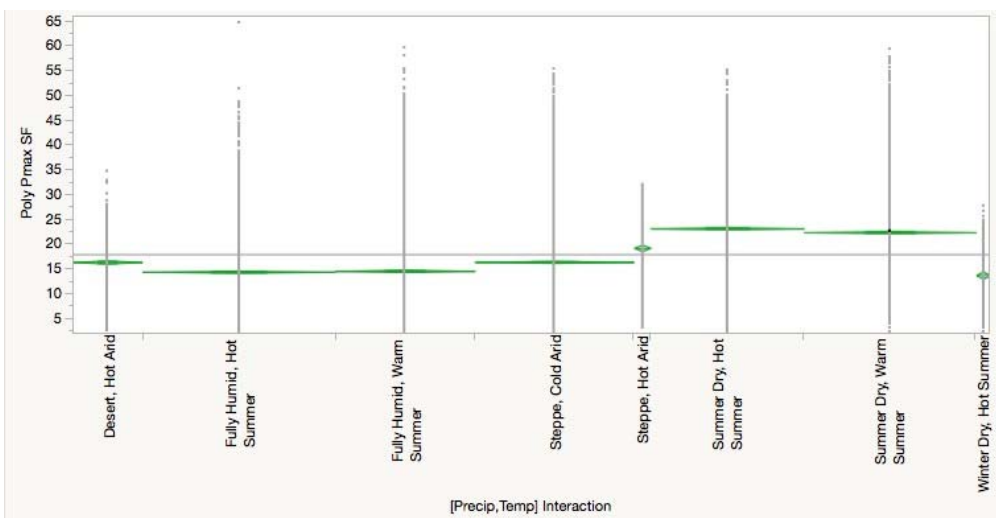

V. CONCLUSION

5.1 Analysis Conclusions

The preliminary analysis completed on the available installation test systems returned results which will be further verified after a full year of analysis. This study was only to verify if the test systems and analysis techniques suggested would perform in practice. The preliminary results comparing the power production capability of the two test panels, which only included limited months of data collection, concluded that the poly-crystalline panels outperformed the mono-crystalline panels for all months and climate classifications. The poly-crystalline panels were more efficient at power production many times by a factor of two when compared to the mono-crystalline panels in the same climate.

The missing and incomplete data sets for many installations made the proper analysis of the climate classifications troublesome. From the data available of the main climate, *Warm Temperate* climates outperformed both *Arid* and *Snow* climates. The only month in which *Warm Temperate* did not have the highest production for both panels was in December. It can be concluded from this that as the seasons change, main climates can change in terms of highest energy producers. This observation gives credence to the need for a full calendar year worth of data before drawing final conclusions.

The analysis of precipitation and temperature factors provided that *Summer Dry* and *Warm Summers* were the highest producing climate. However, just as warm temperate faded in production approaching winter months, these classifications too began to lose efficiency. The incomplete data set unfortunately makes it difficult to discern which climate classifications would then be most productive in the winter months.

The main climate/precipitation interaction saw *Warm Temperate - Summer Dry* installations as having above average production when compared to the mean of all available installations. Likewise, *Summer Dry - Warm Summer* and *Summer Dry - Hot Summer* provided above average production for the precipitation/temperature interactions. These results were as expected.

It is important to reiterate that these results are preliminary. When all installations are operational and a full calendar year worth of data is available to account for seasonal changes, these results may very well change. If the trends remain constant, the hypothesis can be drawn that poly-crystalline cells will continuously outperform mono-crystalline in terms of production capability. It can also be concluded that in the warmer months of summer and early fall, warmer and dryer climates will outperform all other climates in terms of power production.

5.2 Future Research

Future research possibilities for these systems and this data include analyzing the cost and life cycle analysis portion of the industry. Once definitive power production averages can be gathered as to where US Air Force investment should occur, the ability to estimate with relative certainty payback periods for larger systems or arrays will be possible. The USAF and the DoD as a whole can use this knowledge for resilient renewable energy planning, their goal in the years to come.

Additional analysis may also be completed by using the PVWatts photovoltaic model. The PVWatts model produces estimated power production of photovoltaic arrays using real-time climate data from selected locations. The energy data produced during this study can be directly compared to this model for comparison. This analysis would be able to conclude if the PVWatts model provides reasonable results for the US Air Force to use in the future.

5.3 Study Conclusions

In conclusion, this research should be viewed as a proof of concept. The test system design has proven capable in the field. The data gathered over a limited number of months from 25 of the 37 test sites shows validity with expected and hypothesized results. Poly-crystalline panels have produced consistently higher power averages when compared to mono-crystalline panels. This trend, if proved correct, would contrast available literature on the topic. The data gathering and analysis will continue for a period of no less than an entire calendar year with the option of continual data analysis from then on. At the end of the calendar year, the goal is for all installation test sites have test systems installed and continuously gathering data. At this point, further analysis will be run to provide more effective and inclusive conclusions on the most efficient climate classifications for USAF solar power investment.

Bibliography

[1] AIR FORCE INSTRUCTION AFI 32-7063. AIR INSTALLATIONS COMPATIBLE USE ZONES PROGRAM, 2015.

[2] Adil Al-mumin and Abdullah Al-mohaisen. Greening the Kuwaiti Houses : Studying the Potential of Photovoltaics for Reducing the Electricity Consumption Greening the Kuwaiti Houses : Studying the Potential of Photovoltaics for Reducing the Electricity Consumption. (March), 2015.

[3] A. Al-Otaibi, A. Al-Qattan, F. Fairouz, and A. Al-Mulla. Performance evaluation of photovoltaic systems on Kuwaiti schoolsrooftop. *Energy Conversion and Management*, 95:10, 2015.

[4] Morgan Baziliana. Re-considering the E conomics of Photovoltaic Power Morgan Bazilian. *Renewable energy*, 53:329–338, 2013. ISSN 09601481. doi: 10.1016/j.renene.2012.11.029.

[5] Christoph Beck, Juergen Grieser, Markus Kottek, Franz Rubel, and Bruno Rudolf. Characterizing global climate change by means of Koeppen climate classification. *Climate Status Report 2005*, (January):10, 2006.

[6] Michal Belda, Eva Holtanová, TomÅ Halenka, and Jaroslava Kalvová. Climate classification revisited: From Köppen to Trewartha. *Climate Research*, 59(1):1–13, 2014. ISSN 0936577X. doi: 10.3354/cr01204.

[7] Christian Breyer, Alexander Gerlach, Oliver Beckel, and J??rgen Schmid. Value of solar PV electricity in MENA region. *2010 IEEE International Energy Conference and Exhibition, EnergyCon 2010*, (December):558–563, 2010. doi: 10.1109/ENERGYCON.2010.5771744.

[8] H Broesamle, H Mannstein, C Schillings, and F Trieb. Assessment of Solar Electricity Potentials in North Africa Based on Satellite Data and a Geographic Information System. 70(1):1–12, 2001.

[9] Christopher P Cameron, William E Boyson, and Daniel M Riley. Comparison of Pv System Performance-Model Predictions With Measured Pv System Performance. pages 2–7, 2008.

[10] Capt John Nussbaum. *ANALYZING THE VIABILITY OF PHOTOVOLTAIC PAVEMENT SYSTEMS: A STUDY IN STRUCTURAL TESTING METHODS, MEASURING POTENTIAL POWER, AND QUANTIFYING THE RISKS OF IMPLEMENTATION*. Master’s thesis, 2017.

[11] Dissertation Collection. Operation Solar Eagle : a study examining photovoltaic (PV) solar power as an electrical power generation infrastructure NAVAL POSTGRADUATE. 2005.

[12] W. De Soto, S. A. Klein, and W. A. Beckman. Improvement and validation of a model for photovoltaic array performance. *Solar Energy*, 80(1):78–88, 2006. ISSN 0038092X. doi: 10.1016/j.solener.2005.06.010.

[13] Haris Doukas, Konstantinos D. Patlitzianas, Argyris G. Kagiannas, and John Psarras. Renewable energy sources and rationale use of energy development in the countries of GCC: Myth or reality? *Renewable Energy*, 31(6):755–770, 2006. ISSN 09601481. doi: 10.1016/j.renene.2005.05.010.

[14] Solar Energy. Enlisting the sun. (July 1988):1988–1989, 2013.

[15] US Department of Energy. Nellis Air Force Base solar array provides model for renewable projects, 2010. URL https://energy.gov/articles/ nellis-air-force-base-solar-array-provides-model-renewable-projects.

[16] P. Faine, Sarah R. Kurtz, C. Riordan, and J. M. Olson. The influence of spectral solar irradiance variations on the performance of selected single-junction and multijunction solar cells. *Solar Cells*, 31(3):259–278, 1991. ISSN 03796787. doi: 10.1016/ 0379-6787(91)90027-M.

[17] A Hunter Fanney, Brian P Dougherty, and Mark W Davis. Comparison of Predicted to Measured Photovoltaic Module Performance. *Journal of Solar Energy Engineering*, 131(2):021011, 2009. ISSN 01996231. doi: 10.1115/1.3090826.

[18] Air Force and Renewable Energy. AFCEC Energy Directorate. 2015.

[19] Martin A. Green, Keith Emery, Yoshihiro Hishikawa, Wilhelm Warta, and Ewan D. Dunlop. Solar cell efficiency tables (Version 45). *Progress in Photovoltaics: Research and Applications*, 23(1):1–9, 1 2015. ISSN 10627995. doi: 10.1002/pip.2573. URL http://doi.wiley.com/10.1002/pip.2573.

[20] Ali Hajiah, Tamer Khatib, K. Sopian, and M. Sebzali. Performance of grid-connected photovoltaic system in two sites in kuwait. *International Journal of Photoenergy*, 2012, 2012. ISSN 1110662X. doi: 10.1155/2012/178175.

[21] R. R. Hernandez, S. B. Easter, M. L. Murphy-Mariscal, F. T. Maestre, M. Tavassoli, E. B. Allen, C. W. Barrows, J. Belnap, R. Ochoa-Hueso, S. Ravi, and M. F. Allen. Environmental impacts of utility-scale solar energy. *Renewable and Sustainable Energy Reviews*, 29:766–779, 2014. ISSN 13640321. doi: 10.1016/j.rser.2013.08.041. URL http://dx.doi.org/10.1016/j.rser.2013.08.041.

[22] Lion Hirth. Market value of solar power: Is photovoltaics cost-competitive? *IET Renewable Power Generation*, 9(1):37–45, 2015. ISSN 1752-1416. doi:

10.1049/iet-rpg.2014.0101. URL http://digital-library.theiet.org/content/journals/10.1049/iet-rpg.2014.0101.

[23] D C Jordan, J H Wohlgemuth, and S R Kurtz. Technology and climate trends in pv module degradation. *27th European Photovoltaic Solar Energy Conference and Exhibition*, (October):3118–3124, 2012. ISSN 1099-159X. doi: 10.4229/27thEUPVSEC2012-4DO.5.1.

[24] Tamer Khatib, Hussian Kazem, K Sopian, Frank Buttinger, Wilfried Elmenreich, and Ahmed Said Albusaidi. Effect of Dust Deposition on the Performance of Multi-Crystalline Photovoltaic Modules Based on Experimental Measurements. *International Journal of Renewable Energy Research (IJRER)*, 3(4):850–853, 2013. ISSN 1309-0127.

[25] David L King, Jay a Kratochvil, and William E Boyson. Photovoltaic array performance model. *Online*, 8(December):1–19, 2004. ISSN 09270248. doi: 10.2172/919131. URL http://mauisolarsoftware.com/MSESC/PerfModel2003.pdf.

[26] D.L. King. Photovoltaic Module and Array Performance Characterization Methods for All System Operating Conditions. *Review Literature And Arts Of The Americas*, pages 1–22, 1997. ISSN 0094243X. doi: 10.1063/1.52852.

[27] Rory L Klinger. Solar Energy and Asphalt THE FUTURE IS BRIGHT FOR SOLAR ENERGY AND ASPHALT PAVEMENTS. pages 1–2, 2016.

[28] Markus Kottek, Jrgen Grieser, Christoph Beck, Bruno Rudolf, and Franz Rubel. World map of the Köppen-Geiger climate classification updated. *Meteorologische Zeitschrift*, 15(3):259–263, 2006. ISSN 09412948. doi: 10.1127/0941-2948/2006/0130.

[29] M. Koussa, M. Haddadi, D. Saheb, A. Malek, and S. Hadji. Sun tracker systems effects on flat plate photovoltaic PV systems performance for different sky states: A case of an arid and hot climate. *Energy Procedia*, 18:839–850, 2012. ISSN 18766102. doi: 10.1016/j.egypro.2012.05.098. URL http://dx.doi.org/10.1016/j.egypro.2012.05.098.

[30] Irina Mahlstein, John S. Daniel, and Susan Solomon. Pace of shifts in climate regions increases with global temperature. *Nature Climate Change*, 3(8):739–743, 2013. ISSN 1758-678X. doi: 10.1038/nclimate1876. URL http://www.nature.com/doifinder/10.1038/nclimate1876.

[31] Monto Mani and Rohit Pillai. Impact of dust on solar photovoltaic (PV) performance: Research status, challenges and recommendations. *Renewable and Sustainable Energy Reviews*, 14(9):3124–3131, 2010. ISSN 13640321. doi: 10.1016/j.rser.2010.07.065. URL http://dx.doi.org/10.1016/j.rser.2010.07.065.

[32] Bill Marion. Overview of the PV Module Model in PVWatts. *PV Performance Modeling Workshop*, 2010. URL http://www.nrel.gov/docs/fy10osti/49607.pdf.

[33] Jennifer McCabe. Nellis AFB to add second large solar plant. URL http://www.af.mil/News/Article-Display/Article/486227/nellis-afb-to-add-second-large-solar-plant/.

[34] S. Mekhilef, R. Saidur, and M. Kamalisarvestani. Effect of dust, humidity and air velocity on efficiency of photovoltaic cells. *Renewable and Sustainable Energy Reviews*, 16(5):2920–2925, 2012. ISSN 13640321. doi: 10.1016/j.rser.2012.02.012. URL http://dx.doi.org/10.1016/j.rser.2012.02.012.

[35] MikRik. Ultimate Guide To Raspberry Pi. *Computer Shopper*, February, 2015. URL http://micklord.com/foru/RaspberryPiPagesfromComputerShopper2015-02.pdf.

[36] Amy Nagengast, Chris Hendrickson, and H. Scott Matthews. Variations in photovoltaic performance due to climate and low-slope roof choice. *Energy and Buildings*, 64:493–502, 2013. ISSN 03787788. doi: 10.1016/j.enbuild.2013.05.009. URL http://dx.doi.org/10.1016/j.enbuild.2013.05.009.

[37] National Physics Laboratory. When do the four seasons officially begin? (FAQ - Time) : FAQs : Reference : National Physical Laboratory, 2014. URL http://www.npl.co.uk/science-technology/time-frequency/time/faqs/when-do-the-four-seasons-officially-begin-(faq-time).

[38] Bhubaneswari Parida, S. Iniyan, and Ranko Goic. A review of solar photovoltaic technologies. *Renewable and Sustainable Energy Reviews*, 15(3):1625–1636, 2011. ISSN 13640321. doi: 10.1016/j.rser.2010.11.032. URL http://dx.doi.org/10.1016/j.rser.2010.11.032.

[39] Anthony Patt, Stefan Pfenninger, and Johan Lilliestam. Vulnerability of solar energy infrastructure and output to climate change. *Climatic Change*, 121(1):93–102, 2013. ISSN 01650009. doi: 10.1007/s10584-013-0887-0.

[40] Md.Mizanur Rahman, Md. Aminul Islam, A.H.M. Zadidul Karim, and Asraful Haque Ronee. Effects of Natural Dust on the Performance of PV Panels in Bangladesh. *International Journal of Modern Education and Computer Science*, 4(10):26–32, 2012. ISSN 20750161. doi: 10.5815/ijmecs.2012.10.04.

[41] Saifur Rahman, M. A. Khallat, and B. H. Chowdhury. A discussion on the diversity in the applications of photovoltaic systems, 1988. ISSN 15580059.

[42] C. Riordan and R. Hulstron. What is an air mass 1.5 spectrum? [solar cell performance calculations]. *IEEE Conference on Photovoltaic Specialists*, pages 1085–1088, 1990. ISSN 01608371. doi: 10.1109/PVSC.1990.111784.

[43] Franz Rubel and Markus Kottek. Observed and projected climate shifts 1901-2100 depicted by world maps of the Köppen-Geiger climate classification. *Meteorologische*

Zeitschrift, 19(2):135–141, 2010. ISSN 09412948. doi: 10.1127/0941-2948/2010/0430.

[44] E. Skoplaki and J. A. Palyvos. On the temperature dependence of photovoltaic module electrical performance: A review of efficiency/power correlations. *Solar Energy*, 83 (5):614–624, 2009. ISSN 0038092X. doi: 10.1016/j.solener.2008.10.008. URL http://dx.doi.org/10.1016/j.solener.2008.10.008.

[45] Y. Sukamongkol, S. Chungpaibulpatana, and W. Ongsakul. A simulation model for predicting the performance of a solar photovoltaic system with alternating current loads. *Renewable Energy*, 27(2):237–258, 2002. ISSN 09601481. doi: 10.1016/S0960-1481(02)00002-2.

[46] Yan-wei Sun, Angela Hof, Run Wang, Jian Liu, Yan-jie Lin, and De-wei Yang. GIS-based approach for potential analysis of solar PV generation at the regional scale: A case study of Fujian Province. *Energy Policy*, 58(2013):248–259, 2013. ISSN 03014215. doi: 10.1016/j.enpol.2013.03.002. URL http://linkinghub.elsevier.com/retrieve/pii/S0301421513001560.

[47] J. Tovar, F. J. Olmo, and L. Alados-Arboledas. One-minute global irradiance probability density distributions conditioned to the optical air mass. *Solar Energy*, 62(6):387–393, 1998. ISSN 0038092X. doi: 10.1016/S0038-092X(98)00035-8.

[48] Fung Po Tso, David R. White, Simon Jouet, Jeremy Singer, and Dimitrios P. Pezaros. The Glasgow raspberry Pi cloud: A scale model for cloud computing infrastructures. *Proceedings - International Conference on Distributed Computing Systems*, (February):108–112, 2013. ISSN 1545-0678. doi: 10.1109/ICDCSW.2013.25.

[49] Vladimir Vujović and Mirjana Maksimović. Raspberry Pi as a Wireless Sensor node: Performances and constraints. *2014 37th International Convention on Information and Communication Technology, Electronics and Microelectronics, MIPRO 2014 - Proceedings*, (June 2015):1013–1018, 2014. ISSN 00457906. doi: 10.1109/MIPRO.2014.6859717.

[50] Tieling Zhang, Richard Dwight, and Khaled El-akruti. Engineering Asset Management - Systems, Professional Practices and Certification. 2015. ISSN 21954364. doi: 10.1007/978-3-319-09507-3. URL http://link.springer.com/10.1007/978-3-319-09507-3.

[51] Jianhua Zhao, Aihua Wang, Martin A. Green, and Francesca Ferrazza. 19.8% efficient honeycomb textured multicrystalline and 24.4% monocrystalline silicon solar cells. *http://oasc12039.247realmedia.com/RealMedia/ads/click lx.ads/www.aip.org/pt/adcenter/pdfcover test/L-37/1923910458/x01/AIP-PT/APL ArticleDL 1217/scilight717-1640x440.gif/434f71374e315a556e61414141774c75?x*, 10 1998. doi: 10.1063/1.122345. URL http://aip.scitation.org/doi/abs/10.1063/1.122345.

[52] K Zweibel, J Mason, and V Fthenakis. By 2050 solar power could end US dependence on foreign oil and slash greenhouse gas emissions. *Scientific American*, 298(1):64–+, 2008. ISSN 00368733. doi: 10.1038/scientificamerican0108-64. URL http://search.ebscohost.com/login.aspx?direct=true&db=inh&AN=10148322&site=ehost-live&scope=site.

REPORT DOCUMENTATION PAGE	*Form Approved* *OMB No. 0704-0188*

The public reporting burden for this collection of information is estimated to average 1 hour per response, including the time for reviewing instructions, searching existing data sources, gathering and maintaining the data needed, and completing and reviewing the collection of information. Send comments regarding this burden estimate or any other aspect of this collection of information, including suggestions for reducing the burden, to Department of Defense, Washington Headquarters Services, Directorate for Information Operations and Reports (0704-0188), 1215 Jefferson Davis Highway, Suite 1204, Arlington, VA 22202-4302. Respondents should be aware that notwithstanding any other provision of law, no person shall be subject to any penalty for failing to comply with a collection of information if it does not display a currently valid OMB control number.

PLEASE DO NOT RETURN YOUR FORM TO THE ABOVE ADDRESS.

1. REPORT DATE *(DD-MM-YYYY)*	2. REPORT TYPE	3. DATES COVERED *(From - To)*
22-03-2018	Master's Thesis	September 2017- March 2018

4. TITLE AND SUBTITLE

A method to determine the viability of photovoltaic systems in various climate regions

5a. CONTRACT NUMBER

5b. GRANT NUMBER

5c. PROGRAM ELEMENT NUMBER

6. AUTHOR(S)

Applebee, Joseph, A, Capt

5d. PROJECT NUMBER

5e. TASK NUMBER

5f. WORK UNIT NUMBER

7. PERFORMING ORGANIZATION NAME(S) AND ADDRESS(ES)

Air Force Institute of Technology
Graduate School of Engineering and Management (AFIT/EN)
2950 Hobson Way
Wright-Patterson AFB OH 45433-7765

8. PERFORMING ORGANIZATION REPORT NUMBER

AFIT-ENV-MS-18-M-174

9. SPONSORING/MONITORING AGENCY NAME(S) AND ADDRESS(ES)

Mr Robert T. Bossert, Jr.
National Guard Bureau/Operations Division (NGB/A4OC)
3500 Fetchet Avenue
Joint Base Andrews, MD 20762
(701) 857-4350 Robert.t.bossert.civ@mail.mil

10. SPONSOR/MONITOR'S ACRONYM(S)

11. SPONSOR/MONITOR'S REPORT NUMBER(S)

12. DISTRIBUTION/AVAILABILITY STATEMENT

Approved for public release. Distribution is unlimited.

13. SUPPLEMENTARY NOTES

This work is declared a work of the U.S. Government and is not subject to copyright protection in the United States.

14. ABSTRACT

The purpose of this study is to manufacture and disseminate 37 photovoltaic test systems which will be located at various United States Air Force installations worldwide. The Air Force's goals in renewable energy are to determine the potential for systems to aid in promoting resiliency for an installation's energy demands. The test systems are designed to collect climate and power production data from each test site and associated photovoltaic cells. The overall goal of the test system data collection is to determine the correlation between power output of photovoltaic panels and the associated geographic region climate classification. This study does not include a complete analysis of the data as a full year of data has not yet been recorded. A full year of data, including all four seasons, is required for a proper analysis to be completed. The conclusion which can be drawn from this study is that the test systems performed as expected. Not including hardware malfunctions, the systems were able to measure all data as designed. Analysis was able to be completed on four months data which provided initial results and observations on the climate region's performance

15. SUBJECT TERMS

CLimate Classification, Photovoltaics, Renewable Energy,

16. SECURITY CLASSIFICATION OF: a. REPORT	b. ABSTRACT	c. THIS PAGE	17. LIMITATION OF ABSTRACT	18. NUMBER OF PAGES	19a. NAME OF RESPONSIBLE PERSON
U	U	U	UU	64	Dr. Diedrich Prigge, AFIT/ENV
					19b. TELEPHONE NUMBER *(Include area code)* diedrich.prigge@afit.edu

Standard Form 298 (Rev. 8/98)
Prescribed by ANSI Std. Z39.18